3

REYST

Master Thesis

Reservoir Modelling of Low Temperature Geothermal systems

Author:
Yapi Donatien Achou

Supervisor:
Dr. Gudni Axelsson

A thesis submitted in fulfilment of the requirements for the degree of Master of Science. 30 ECTS credits

.

May 2014

"The end of a matter is better than its beginning; Patience of spirit is better than haughtiness of spirit."

Ecclesiates 7 : 8

Acknowledgements

I would like to say thank you to my supervisors for their patience, and all the faculties and staff in REYST who gave me the opportunity to complete this work
. . .

Contents

List of Figures

List of Tables

Chapter 1

Introduction

In an increasing world population, energy consumption is directly linked to the survival of the human specie. With three quarter of the world energy source coming from fossil fuel in 2004 [25], the world is subjected to an environmental crisis linked to our energy sources. The need for clean and renewable energy has never been important as it is today. Geothermal energy classified as clean and sustainable energy has the potential of contributing significantly to sustainable energy use in many parts of the world [2]. Generated by radioactive elements in the crust and lava within the earth, geothermal energy provides an unlimited source of energy for the world population.

Geothermal energy production at a sustainable rate can be maintained for $100-300$ years [2, 4]. This requires knowledge and understanding of the geothermal system, sustainable production schemes such as reinjection of cold water and good management strategies. These strategies involve a multidisciplinary field of studies comprising geology, geophysics, chemistry and mathematics. With the development of modern computer architectures, numerical simulation combined with geological, geophysical and chemical data, play a key role in geothermal resource management.

Many pioneering works have been done in the field of geothermal engineering. Axelsson, Barker and Stefansson presented reinjection of water as a resource management strategy [2, 3, 8, 13, 53]. A method for analysing tracer test data used in reinjection was derived by Axelsson et. al [3]. A lumped parameter modelling technique was developed by Axelsson to simulate pressure response due to production in a low temperature geothermal system [11, 12]. Bjornsson developed the well bore simulator HOLA capable of simulating steady state two phase flow in a multi feed zones geothermal well [17]. Bodvarson was the first to derive an analytical method for calculating the thermal front velocity induced during injection of cold water in a hot geothermal reservoir for constant rock and fluid properties [19]. His method was latter extended for temperature independent rock and fluid properties by Stoppa et al and Achou [1, 57].

The main objective of this study is to present different methods used in modelling geothermal systems, in particular low temperature geothermal systems. volumetric and dynamic methods are presented. Reinjection is presented as an essential part of sustainable production of geothermal energy. The lumped parameter modelling method is applied to a low temperature geothermal reservoir located in Munadarnes in west Iceland. The simulation reveals that the reservoir permeability is high. Multiple reinjection scenarios with different production and reinjection rate show that reinjection increases significantly the pressure of the reservoir. By using an analytical solution of water flow in a one dimension channel, the cooling response of the production well due to injection of cold water is presented. Cooling is minimised by placing the reinjection well at a few km from the production well. By revisiting the work of Stoppa et. al [57], an analytical method based on the theory of conservation laws is used to derived the thermal front velocity induced by reinjection.

The thesis is organised as follows: In chapter 2, properties of hydrothermal and geothermal systems are discussed. Hydrological and thermal properties of hydrothermal systems are presented. Geothermal systems are classified and methods for geothermal resource assessment are presented. In chapter 3, the thermal front velocity of cold water is derived using an analytical method. Chapter 4 present a case study using lumped parameters modelling. Chapter 5 contains conclusions and discussion and the possible extension or improvement of this work.

Chapter 2

Background

2.1 Hydrothermal system

Hydrothermal systems can be defined as a set of processes that redistribute energy and mass in response to fluid circulation [43]. Hydrothermal systems includes heat, fluid and sufficient permeability in the natural geological formation. The heat source is a magma chamber. Less frequently the source of heat is the crust with an abnormal high concentration of radioisotopes, mainly potassium 40, thorium 232, and uranium 235 and 230 [55]. The origin of the fluid is meteoric, that is rain water that percolates the ground, and frequently mixed with fluids and solutes of magnetic origin. In connection to geothermal energy, the most important properties of hydrothermal systems are given by rock and fluid properties. They are: permeability, porosity and storage capacity [5]. The permeability represents viscous interactions between fracture surfaces and the fluid as it flows through interconnected fracture networks [43]. Permeability expresses the ease at witch fluid flows through the medium. It is a qualitative property of the system, while porosity is a quantitative property described bellow.

2.1.1 Hydrological properties

the main hydrological property is porosity. Hydrothermal systems are mainly an interconnection of fracture. However, hydrothermal system can be approximated by porous medium [9].

2.1.1.1 Porous medium

A porous medium is a substance containing voids or pores, allowing fluid to be trapped or to flow throughout the medium. in the contest of geothermal energy, we are interested in the voids within the subsurface geological formation such as rock. To allow fluid flow, the pores spaces must form a network of interconnected voids space. Based on the time they were formed, the pores space can be divided in two, [15]. Original pore spaces are formed during the rock formation while secondary pore spaces are formed after the rock formation. Secondary porosity are due to physical and chemical changes occurring during the conversion of one rock type to an other. Porous medium can be classified based on their constituents. Intragranular porous medium created by voids within the rock grains and Intergranular porous medium formed by the voids between the rock grains. Fracture porosity is due to fractures within the rock caused by tensional forces. On the basis of mechanical properties, we can distinguish between consolidated porosity and unconsolidated porosity. In the consolidated case, the grains are kept together with a cementing material, while in the unconsolidated case the grains are loose, [15].
Matrix porosity as a statistical measure of the voids spaces with respect to the total rock volume can be expressed as

$$\Phi = \frac{V_T}{V_T} = 1 - \frac{V_S}{V_T}$$

where

$$V_T = V_S + V_P$$

is the total porosity, V_P, V_S are the pore volume and solid (rock) volume respectively. In geothermal systems, only effective porosity is of importance, because it reflects interconnected pores and allow fluid to flow, [9]. Effective porosity affects the storage capacity of the medium, which is its ability to absorb or release fluid in response of pressure change, due to fluid extraction or fluid injection in the medium. Alternatively we can define fracture porosity as the fraction of volume occupied by fractures.

The recharge mechanism of porous medium are partly due to precipitation from the highland, that infiltrate the ground under gravity, filling up the interconnected

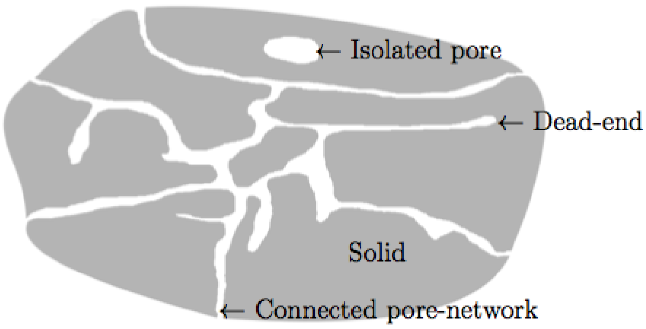

FIGURE 2.1: A porous medium with connected network of pores, from [24]

pores spaces to form a saturation zone, [15]. When a part of the porous medium is trapped between impermeable formation, it is termed confined. Alternatively, an unconfined aquifer is bounded above by a water table. The movement of cold water in porous medium is described by Darcys law

2.1.1.2 Darcys law

Henry Darcy was a French hydraulic engineer interested in purifying water supplies using sand filters. He conducted experiments to determine the flow rate of water through the filters. Published in 1856, his conclusions have served as the basis for all modern analysis of ground water flow.The motion of cold water in porous medium is described by Darcys law:

$$Q = -K\frac{\rho}{\mu}(\Delta P - \rho g)$$

where

$$K = \begin{bmatrix} K_x & 0 & 0 \\ 0 & K_y & 0 \\ 0 & 0 & K_z \end{bmatrix}$$

is the permeability tensor in 3 dimension. $Q(kg/sm^2)$ is the fluid flow rate, $\Delta P(Pa/m)$ the pressure gradient, g acceleration of gravity and μ the fluid kinematic viscosity. Darcys law stipulates that the motion of cold water in porous medium is due to the difference in pressure between two points and/or gravity forces. Capillarity pressure are pressure associated with low porosity, and can be neglected if we assume that fluid is flowing through the porous medium. Darcys law hold for laminar flow characterised by

$$R_e = \frac{Vd}{\nu}, \quad 1 \leq R_e \leq 10$$

where d is the flow path diameter and R_e the Reynolds number. Darcys law hold in porous medium but also in fracture medium, since large scale fracture medium can be approximated by porous medium, [9]. The pore velocity v or the interstitial velocity is related to Darcy law by dividing the flow rate Q by the porosity ϕ. The pore velocity would be the velocity a conservative tracer would experience if carried by the fluid through the formation

$$v = \frac{Q}{\Phi}$$

2.1.2 Thermal properties

As mention before, about 80% of the earth energy is generated by the decay of unstable radio active elements in the crust and the mantle, [32]. The major heat producing elements are Uranium-238, Uranium-235, Potassium-40, and thorium-232

elements	Heat generation (W/kg^{-1})	Quatity (ppb)	Summary
Uranium	$9.8.10^{-5}$	15-25	Uranium-238 produces 99.28% of the total Uranium energy. Uranium-235 produce 0.72% of the total energy produce by Uranium.
Thorium	$2.6.10^{-5}$	80-100	Thorium-232 one out of 10^4
Potassium	$3.35.10^{19}$	150-260	Potassium generate more energy per kg.

TABLE 2.1: Heat producing radioactive elements, [32]

The Crust generate 100 time more energy than the mantle per unit volume. However, the rate of energy generation for the entire earth is influenced by the mantle due to it large volume relatively to the crust, where the fifth of radioactive heat is generated. The total energy of the crust is about $1.4-2.7.10^{13}W$ [32]. Due to low matrix and fracture porosity, about 80 to 90% of this energy is stored in the rocks, [18]. The energy generated is mostly transfer through convection and conduction. Radiation is ignored in modelling heat and mass extraction in hydrothermal systems. However, radiation plays an important role in shock wave propagation in hydrothermal systems. Hot fluid moves in the system through convective cells, where fractures are predominant.
consider a volume V_c, V_h of cold and hot water respectively, and associated mass m_c, m_h. Assume that the fluid is heated bellow. The density of fluid is given by

$$\rho = \rho_0[1 - \alpha(T - T_0) + \beta(P - P_0)].$$

where the compressibility

$$\beta = -\frac{1}{\rho}\frac{d\rho}{dp} = -\frac{1}{V}\frac{dV}{dp}.$$

and α is the extensibility. The density decreases with increasing temperature, therefore

$$m_h = \rho_h V_h \leq \rho_c V_c = m_c.$$

The column of hot water will rise when it is heated bellow. As it rises away from the heat source, it temperature decrease and the density of the fluid increase, allowing the column of cold water to fall. This create a convective cell. Many such cells are responsible for heat transfer in fractured porous medium.

When rock within the upper mantle and the crust are partially melted, the resulted molten lava, with lower density rises toward shallower depth in the form of magma chamber, dykes, or volcanics discharge, [50].
Conduction is predominant in sedimentary systems, where due to sediments packed together, fractures are more scarcer. in those systems, the microscopic particles undergoes constant oscillations and collisions. The energy generated by this chaotic

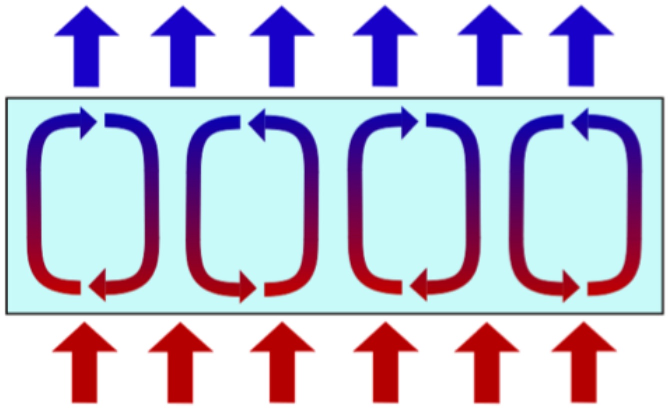

FIGURE 2.2: A convective cell heated from bellow, from [24]

movement create a temperature gradient causing heat to flow smoothly from region of higher temperature to region of low temperature. This is expressed by Fourier law

$$q = -k\Delta T \tag{2.1}$$

where q, k, T are the heat flux, rock thermal conductivity and temperature respectively. Unlike conduction which generates smooth temperature field, radiation generate jump in the temperature field due to shock wave propagation.

2.2 Geothermal Systems

Geothermal energy can be defined as the outward energy flux of the earth, stored in the crust. The decay of unstable radio active elements such as Thorium, potassium and Uranium are for the most part responsible for this energy [32]. Most geothermal systems are located along plate tectonics and are associated with volcanic regions. Due to a natural geothermal gradient within the crust, geothermal energy can a priori be found anywhere on earth.

A geothermal field is a geographical area with geothermal activity at the earth surface [10]. All hydrological systems directly related to geothermal resources such as fractures zone, heat source, aquifers etc... constitute the geothermal system. The geothermal reservoir is the permeable and hot part of the system [10]. Geothermal systems are classified on the basis of temperature (enthalpy) and their geological setting.

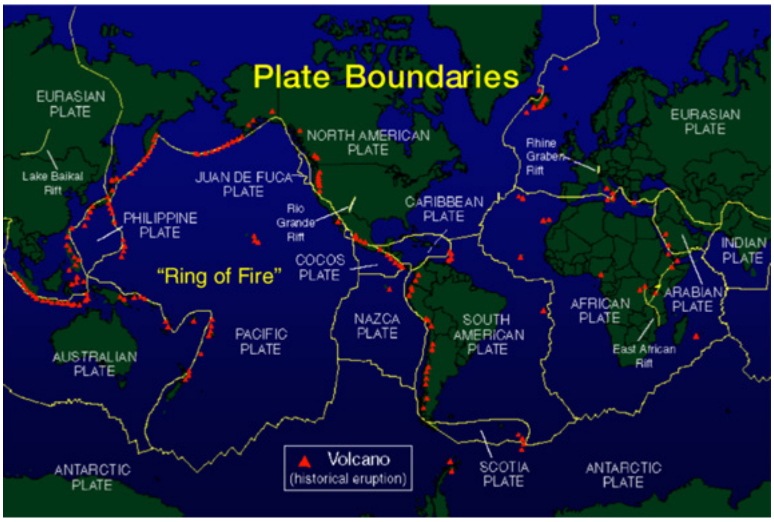

FIGURE 2.3: Geothermal systems and plate boundaries

2.2.1 Classification based on temperature

On the basis of temperature, geothermal systems can be classified as high temperature systems and low temperature systems. The temperature is at least 200 °c in high temperature systems, while low temperature systems are characterised by temperature below 150 °c [10]. The heat source in high temperature systems is often a hot intrusive magma, formed by incomplete melting of the upper mantle and the crust. High temperature systems are generally situated in volcanic regions. The heat source in low temperature systems, is the hot crust heated by radioactive elements.

2.2.2 Classification based on geological formation

On the basis of their geological setting, conventional geothermal systems can be classified as volcanic systems, convective systems, sedimentary systems, Engineered Geothermal Systems (EGS) and shallow geothermal systems [10].

Volcanic systems are located within or in the proximity of volcanic complexes. They are high temperature systems and two phase flow (liquid and steam). The flow of water in volcanic systems is controlled by permeable fractures and fault zones [10]. The heat sources are hot intrusions or magma [10]. *Convective systems* are often situated outside volcanics complex and are predominantly low temperature systems. Characterised by highly fractured rocks heat is transferred within a convective system through convection cells. *Sedimentary systems* are located in sedimentary basins characterised by permeable sedimentary layers. Heat is transfer mainly through conduction [10]. An *engineered geothermal system* generate geothermal energy without the need for natural convective hydrothermal resources. Through hydraulic stimulation, high pressure cold water is injected into the system, to enhance permeability in the naturally fracture rock. *Shallow geothermal systems* refer to the thermal energy stored near the surface of the earth crust. This energy is utilised through heat pumps.

Recently abandoned oil and gas wells or dry wells have been investigated for possible sources of geothermal energy. Abandoned oil and gas wells are wells that ceased or never produced oil and gas. They can be as deep as 6000 m [27] In most geothermal project the cost of drilling can be as high as 50 % of the total project cost [26]. By using abandoned oil and gas wells, the cost of geothermal energy production is reduced significantly. To produce geothermal energy from abandoned oil and gas wells, a double pipe heat exchanger is inserted into a well see Figure 2.4.

A working fluid is injected in one orifice of the heat exchanger. Due to the

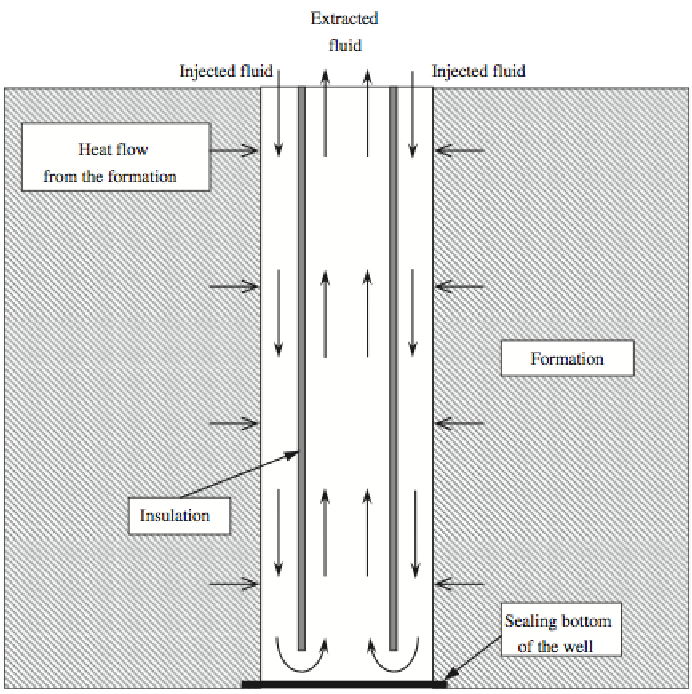

FIGURE 2.4: Diagram of a double pipe heat exchanger

natural geothermal gradient, the fluid is heated by the geological formation. The recover geothermal energy depends on the flow rate of the injected working fluid and the geothermal gradient [26, 27]. Computational simulation indicates that the fluid temperature can be around 130 °c or more [26]. Organic fluid such as isobutane can be used as working fluid. Due to their low boiling point they are easily converted into high temperature steam [27].

2.2.3 Geothermal resource assessment methods

Geothermal engineering is a multidisciplinary field of study. It includes numerical simulation, geophysics, geology and chemistry. The purpose of geothermal reservoir engineering is to estimate reservoir properties and production potential, simulate production response and estimate the size of geothermal resources. It plays a key role in resource management. Assessment methods in geothermal reservoir engineering are divided into two: Volumetric assessment method and dynamics assessment method [36]. Volumetric assessment methods are used in the the first stage of a geothermal project and should be included in conventional geothermal monitoring programs [4, 36, 64]. Volumetric method plays an integral role in geothermal resource management [4]. It includes the use of geological, geophysical and chemical methods. Data from volumetric methods can be used to construct a conceptual model of the reservoir. The conceptual model is a descriptive model of the system. It incorporates the essentials physical features of the system such as heat sources, hot springs, permeable zones, boundary condition, recharge zones etc [47]. The conceptual model provides an estimate of the reservoir size and describes flow pattern within the system. It is the foundation for a successful numerical simulation. Volumetric method plays a key role during production. Dynamical methods includes simple analytical methods, details numerical simulations and lumped parameters modelling [36]. A combination of volumetric methods and numerical simulation should enhance the reliability of mathematical model of geothermal systems [7]

2.2.3.1 Volumetric assessment methods

Geological methods

The most widely used method is geological mapping. It goal is to study the viability of a geothermal project. It includes geothermal surface manifestation mapping, surface petrology, mineralogy, lithology, tectonic. It also plays an import role in advanced stages of the project in well siting and well design. A map of surface thermal manifestation such as hot spring, mud pots and warm group can reveal if the geothermal field is active of extinct [64].

Geophysical methods

Geophysical methods are import part of geothermal resource assessment. Physical parameters such as density, resistivity and magnetism of the rock are measured. Gravity survey is used to measure the density variation, which can reveal dense intrusions. Magnetic measurement can give information about dikes. Seismic surveys and seismic monitoring reveals fracture zones at depth [64]. Gravimetric measurements may reveal tectonic features in the reservoir [64]. Micro gravity monitoring can provide information on the net mass balance of the reservoir (difference between mass withdrawal and the recharge of water) [7]. Mass balance from enlarging steam zones may also be seen from gravity monitoring [7]. Mass balance effect of reinjection may be detected by gravity monitoring [7]. Resistivity surveys reveals temperature distribution of the system and might help delineate cold fresh water inflow into the geothermal system [7]. The commonly used resistivity survey are Transient ElectroMagnetic (TEM) and MagnetoTelluric (MT) sounding [64].

In TEM survey current is generated in a big loop laying on the ground. By induction the current produces a magnetic field in the ground. By turning off the current abruptly, the varying magnetic field in the ground induce a current. This current is used to map the resistivity structure of the upper most 1 km of the geothermal system [64].

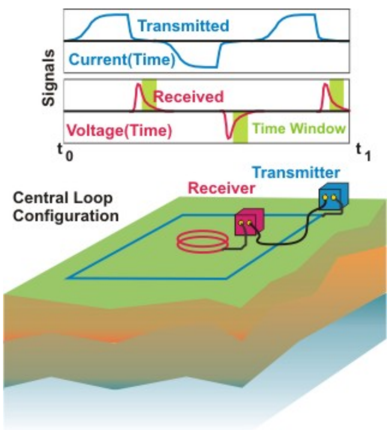

FIGURE 2.5: TEM survey

The TM survey makes use of the natural fluctuation of the earths magnetic field. By the principle of induction, the induced current in the earth is measured on the surface by two magnetics dipoles. Because the TM survey uses the natural magnetic field of the earth, it maps the resistivity structure of the geothermal system at greater depth, tens of km [64].

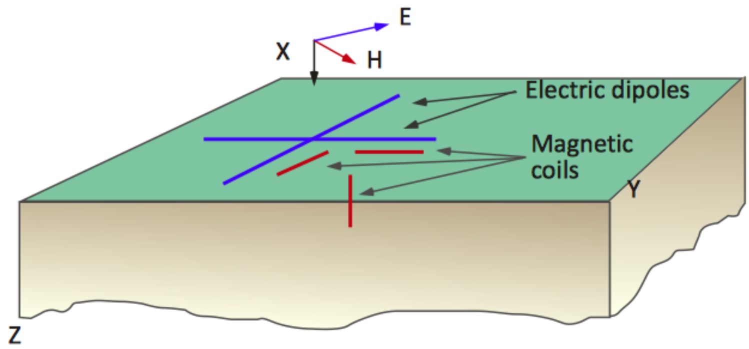

FIGURE 2.6: TM survey

Chemical methods

Chemical composition of geothermal fluid (steam and water) can reveal the temperature of the reservoir. it plays an important role in anticipating corrosion and scaling in pipes and wells by identifying corrosive and scaling species. Chemical composition of the surface water reveals information about the recharge zone of a geothermal reservoir [64]. Change in silica content of water production can be interpreted as inflow of cold water into the geothermal system [7].

2.2.3.2 Dynamics assessment method

Numerical simulation

Traditionally, conceptual models of geothermal systems are developed on the basis of information from various disciplines including geology, geophysics and geochemistry. Mathematical models are then applied to simulate the behaviour of the system using conceptual models [37].

On the basis of the conceptual model constructed from volumetric assessment methods, a careful mathematical model of the reservoir is constructed. Variables such as pressure, enthalpy, saturation, permeability, storage capacity are often simulated. A successful mathematical model is based on deep understanding of

the physical and chemical processes of the system, the boundary condition, the fluid and rock properties, the location of sources and sinks [47]. Fluid flow in geothermal systems can be approximated by flow in a porous medium. The flow is characterised both as single phase (water) with multi-component (carbon-dioxide and NaCl) or multi phase flow consisting of two phases, water and steam [37].
Geothermal systems are modelled in terms of conservation of mass, momentum and energy. A complete model of the system should incorporate the flow of fluid in the reservoir and the production/reinjection wells [37]. The general conservation equations for simulating two phase flow in a geothermal reservoir are given by Grant [35]:

Conservation of mass

$$\phi\frac{\partial}{\partial t}(\rho_l S_l f_l + \rho_g S_g f_g) + \nabla\cdot(\rho_l u_l f_l + \rho_g u_g f_g) + q_m = 0 \tag{2.2}$$

where ρ, S are the saturation and f is the mass concentration of the chemical species in the fluid. l and g stand for liquid and gas (vapour). u is given by equation (2.4,2.5). q_m is the sink/source term (kg)

Conservation of energy

$$\phi\frac{\partial}{\partial t}((1-\phi)\rho_r U_r + \phi(\rho_l S_l U_l + \rho_g S_g U_g)) + \nabla\cdot(\rho_l u_l h_l + \rho_g u_g h_g - K\nabla T) + q_E = 0 \tag{2.3}$$

U is the internal energy, h the enthalpy , T the temperature, K the heat conduction coefficient and q_E the sink/source term $(J/m^3 s)$.

Conservation of momentum

The conservation of momentum is given by Darcys law. It describes a linear relationship between the fluid velocity and the pressure gradient relative to the rock:

$$u_l = -\frac{kk_{rl}}{\mu_l}\nabla(P_l - \rho_l g z) \tag{2.4}$$

$$u_g = -\frac{kk_{rg}}{\mu_g}\nabla(P_g - \rho_g g z) \tag{2.5}$$

k is the absolute permeability, and k_{rl} and k_{rg} are the relative permeabilities of the rock to the liquid and vapour phase respectively. The above equations hold assuming that capillary pressure effects are neglected.

The steady state equation governing fluid flow in a vertical geothermal well is given by the mass, momentum and energy equation [17]

$$\frac{\partial m}{\partial z} = 0 \tag{2.6}$$

$$\frac{\partial P}{\partial z} - \left(\left(\frac{\partial P}{\partial z}\right)_f + \left(\frac{\partial P}{\partial z}\right)_a + \left(\frac{\partial P}{\partial z}\right)_p \right) = 0 \tag{2.7}$$

$$\frac{\partial E}{\partial z} \pm Q = 0 \tag{2.8}$$

where Q is the heat flow and $\left(\frac{\partial P}{\partial z}\right)_f, \left(\frac{\partial P}{\partial z}\right)_a, \left(\frac{\partial P}{\partial z}\right)_p$ are the pressure drop due to frictional, acceleration and potential forces along the well respectively. They are given respectively by

$$\left(\frac{\partial P}{\partial z}\right)_f = \varphi^2 \left(\frac{f_{lo} G^2}{4 r_w \rho_l}\right) \tag{2.9}$$

$$\left(\frac{\partial P}{\partial z}\right)_a = G(x u_g + u_l(1-x)) \tag{2.10}$$

$$\left(\frac{\partial P}{\partial z}\right)_p = (\rho_m) g \tag{2.11}$$

u_l and u_g are the liquid and steam velocity, φ^2 is the two phase multiplier introduced by Martinelli and Nelson:

$$\varphi^2 = 1 + \left(\Gamma^2 - 1\right)\left(B_r x(1-x) + x^2\right)$$

$$\Gamma^2 = \frac{\rho_l}{\rho_g}$$

$$B_r = B_s\left(\frac{1}{2}\left(1 + \left(\frac{\mu_g}{\mu_l}\right)^2 10^{-\frac{300\epsilon}{r_w}}\right)\right)$$

f_{lo} is the liquid friction factor and B_s is given by Table 2.2.

TABLE 2.2: Different values of B_s based on Γ and G

Γ	$G(\frac{kg}{m^2 s})$	B_s
≤ 9.5	≤ 500	4.8
	$500 \leq G \leq 1900$	$\frac{2400}{G}$
	≥ 1900	$\frac{55}{G^{0.5}}$
$9.5 < \Gamma < 28$	≤ 600	$\frac{520}{\Gamma G^{0.5}}$
	> 600	$\frac{21}{\Gamma}$
≥ 28		$\frac{15000}{\Gamma^2 G^{0.5}}$

$$E = m(xh_g + (1-x)h_l + 0.5(xu_g^2 + (1-x)u_l^2) + g(L_w - z)) \tag{2.12}$$

For constant mass flow rate m (3.1, 3.2) can be solved for pressure P and steam quality x by using Newton method for system of nonlinear equations.

Equations governing the behaviour of a geothermal system can be solve numerically by various softwares. Softwares for geothermal systems simulation fall into two categories: Reservoir and wellbore simulation software. The widely reservoir simulator are THOUGH and its family, STAR and TETRAD [36, 48, 49, 56]. THOUGH family are designed to simulate the coupled transport of fluid, heat and chemical species for multi phase flow in porous and fracture media [49]. The conservation equations are discretised in space using the integral finite difference method [30, 37, 42]. The time derivative is discretised using a finite difference scheme (backward, forward, centered). Due to the fact that THOUGH is discretised using an integral finite difference method, it has the advantage of handling unstructured mesh as opposed to STAR and TETRAD. This makes THOUGH the facto reservoir simulation software [36]

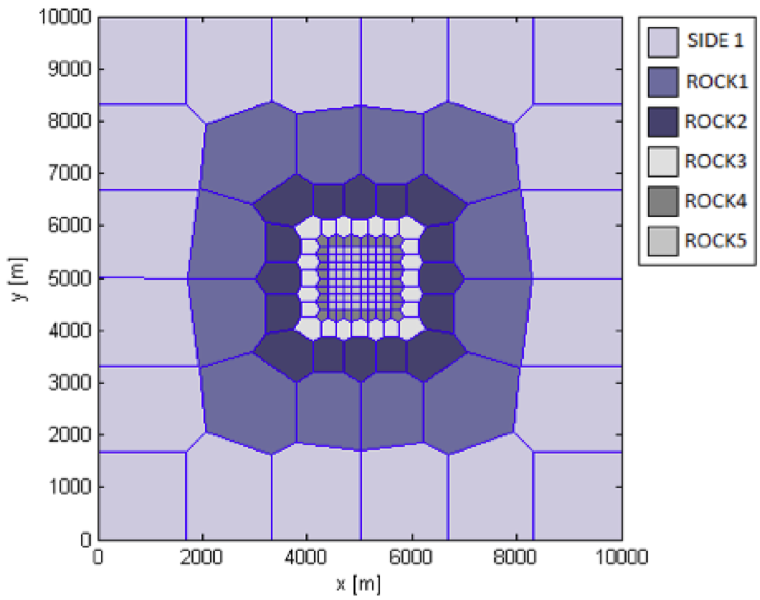

FIGURE 2.7: Unstructured mesh generated by THOUGH2. Taken from [36]

The first wellbore softwares were designed to solve steady state conservation equation [34, 36]. The first simulator capable of handling unsteady state conservation equation was WELBORE designed by Miller [36, 44]. All these softwares solved the conservation equations from bottom to top along the well or vice versa, without incorporating the feed zones in the wells. The first software able to handle one feed zone was the software BROWN [16, 36]. HOLA was the first simulator capable of handling multiple feed zones in the well [17].

A successful geothermal systems simulation is based coupling empirical data and numerical simulation. The verification process map the measured data from the system to the result obtained from mathematical modelling. Verification is done through calibration [47]. If the error between the measured and the calculated solution falls within an acceptable range, the simulation is a success. In this case the mathematical model represents a fairly good approximation of the system. Osulavan developed a general method of model calibration [47]. It consists of natural state modelling followed by history matching. In natural state modelling, the model is run for a long period of time to mimic the natural behaviour of the system. The simulated variables are compared with the measured field data. Some parameters of interest such as permeability structure, location of the heat source of the model are adjusted to obtain the minimum possible discrepancy between measured and simulated data. This step does not take into account the production history of the system. For system with production history, the measured behaviour of the geothermal field is matched with the simulated behaviour in response to production [47].

Lumped parameters modelling and analytical method

A lumped parameter modelling software was designed by Axellsson to simulate the pressure change in a low temperature geothermal well [12]. The methods consist of approximating the permeability and the storage capacity of the reservoir by plumped parameters. By using inverse modelling the analytical response of the reservoir is mapped with measured data. Simple analytical method can also be used to model fluid flow in geothermal reservoir. In Chapter (3) a case study using a lumped parameter modelling approach is presented. In chapter 4 a simple analytical method is used to predicts the thermal front velocity of injected cold water in a hot single phase geothermal reservoir.

2.3 Reinjection in geothermal systems

2.3.1 Historical background and advantages

Reinjection in geothermal resource management consist of reinjecting the used geothermal water back into the reservoir. Water of different origins such as surface water and sewage water can also be reinjected [8]. It started as a way on disposing the wast water from geothermal energy utilisation [8]. The first recorded instance

of injection of cold water into a high temperature reservoir is in Ahuachapan field in El Salvador in 1969 [8, 53]. At the same time a long term reinjection was used successfully in the Dogger limestone reservoir located in the Paris basin [8]. The Dogger reservoir stretching $150000km^2$ is mainly used for district heating. The production and reinjection wells are separated by a distance of about $1km$. The reinjection scheme in the Paris basin lasting 30 to 40 years has indicated no significant cooling of the reservoir due to cold water injection [8]. In 1970, operators in the Geyser geothermal field started to inject the steam condensate, and realised that this process increased the reservoir performance [8]. Since then reinjection has been an integrant part of resource management in the Geyser field. It was latter observed that due to injection, the decline of electrical production in the geyser was considerably slow [8, 52].
In Italy reinjection started in 1974 at Lardelerollo field as a means to dispose the steam condensate [8, 23, 53]. Long term production history has revealed that since reinjection started, steam production along with pressure have increased in the Lardelerollo geothermal field [8, 53], See Figure 2.8.

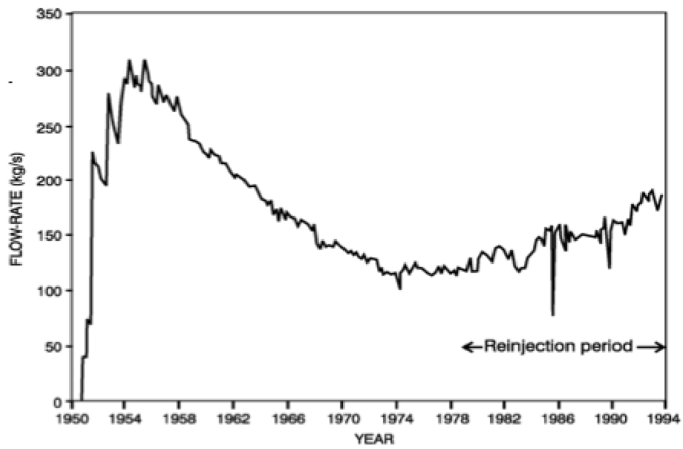

FIGURE 2.8: Flow rate history at the Lardelorro field [23]. Taken from [8]

Reinjection sarted in Iceland in 1997 at the Laugaland low temperature field in north Iceland [7]. In the Laugaland geothermal system 20 to 20% of the extracted mass are reinjected [7, 8]. In the Hofstadir geothermal system in West Iceland reinjection started in 2006. About 40 to 50% of the extracted mass are reinjected back into the system [8]. Due to the low chemical content in most Icelandic geothermal field and the good recharge of water, reinjection started relatively late in Iceland [8]. Now reinjection is practiced in most of the hight temperature field in Iceland. It is estimated that the number of geothermal field in which reinjection is a part of resource management is likely more than 60 [8].

Reinjection is a vital part of an Enhanced Geothermal System (EGS) [8]. An EGS is a man made reservoir, created where there is hot rock but insufficient or little natural permeability or fluid saturation. About 80 to 90% of the energy of a geothermal reservoir is stored in the rock [8, 32]. Therefore in an EGS, fluid is injected into the system at a sufficient pressure to create a fracture network into the rock with sufficient permeability. A production well is drilled into the fracture network to intersect the created flow paths.

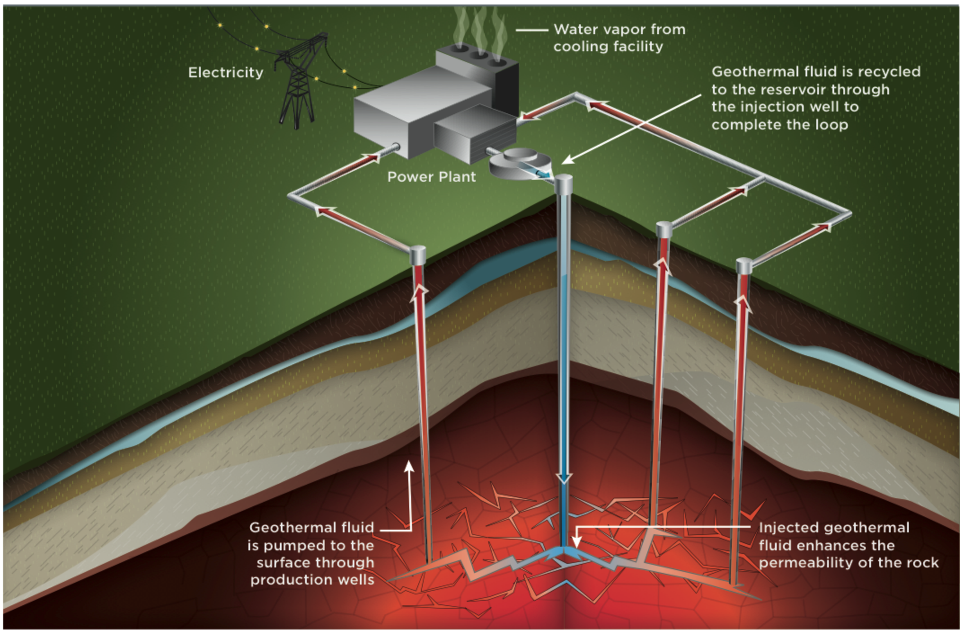

Figure 2.9: schematic description of an EGS

The production capacity of a geothermal system is controled by pressure response [10]. During reinjection, the reservoir pressure is increased significantly, therefore reinjection increase the production capacity of the reservoir. As an environmental protection tool, it is a way of disposing the hight chemical content of geothermal wast water. It mitigates surface subsidence and maintains the integrity of surface activities [8].

Reinjection can however affect the lifetime efficiency of the reservoir. The lifetime efficiency of a reservoir can be defined as the ratio of the heat produced over it life time to the total available heat content of the reservoir [51]. It can written as

$$\eta = \frac{E_r}{E_T}$$

where η is the efficiency, E_r, E_T are the heat produced by the reservoir over it life time and the total available heat content respectively. The injected water is generally colder than the reservoir rock and can intersect fractures to create a premature cold water inflow and cool down the reservoir and decrease the reservoir efficiency. Reinjection can create and reopen pre-existing fractures. If created or reopen fractures intersect a cold aquifer, cold water breakthrough can be induced into the reservoir. Due to a large amount of fluid being injected into the reservoir, pressure increase can cause rock to slip along pre-existing fractures and produce microseismic events. Silica scaling in high temperature system, carbonate scaling in low temperature system and corrosion in pipelines and injection wells can be problems associated with injection. clogging of acquirers next to injection wells in sandstone reservoir can also be a significant problem [8]. To mitigate the problems associated with reinjection , a careful reinjection scheme must be designed.

2.3.2 Mitigating problems associated with reinjection

The main goals of reinjection can be summarise as follow:
1) Counteract pressure decline due to production
2) Maximise the reservoir efficiency by increasing the heat production over the life time of the reservoir
3)Environmental protection scheme

If the purpose is option 3, injection wells can be placed outside the main production field without any direct hydrological connection [8]. If the purpose of the reinjection scheme is option 1 and 2, the rejection wells must be located inside the main production reservoir, in between production wells or on the outskirts of the reservoir but still in direct hydrological connection [8]. To avoid premature thermal breakthrough and increase the efficiency of the reservoir through injection, the injection scheme must ensure the optimum distance between injection wells and production wells [8, 51]. Thermal breakthrough have been observed in relatively few geothermal systems worldwide [8, 53]. In the Palinpinon geothermal system in the Philippines, thermal breakthrough occur about 18 months after reinjection started. The temperature dropped by about 50 °c over a period of 4 years [8]. Tracer tasting can be done to locate fracture zones, flow path and determine the thermal front velocity to predict any premature thermal breakthrough. Analytical method can also be used the determined thermal front velocity. In chapter 4, an analytical method to determine thermal front velocity is presented.

2.3.2.1 Tracer testing

Tracer tests are the most powerful tool for studying connections between injection and production wells and predict thermal breakthrough [6]. It involves injecting a chemical tracer into the geothermal system, and monitor its recovery through time at various points.The chemical tracer arrival time and the thermal breakthrough time are proportional by $2-3$ order of magnitude [8]. Therefore determining the tracer arrival time gives the thermal breakthrough time. Three types of tracer are commonly used in geothermal application: Radioactive tracers such as Iodine-125, Iodide-131, Tritium etc, Fluorescent tracer such as rhodamin WT, chemical tracer such as iodide, bromide etc [3].
Assuming that a tracer of mass M is injected at $t=0$ with injection rate q into a one dimensional channel with cross sectional area A, porosity ϕ and fluid density ρ,

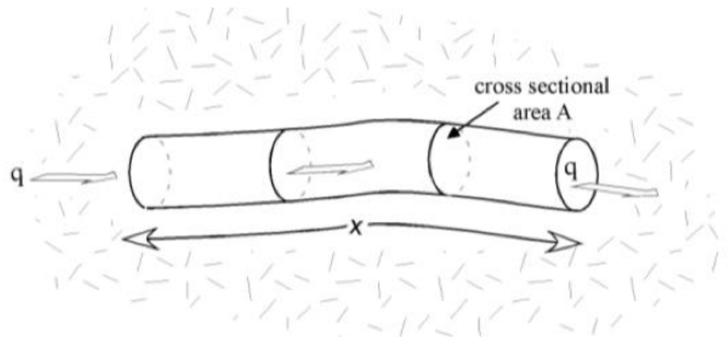

FIGURE 2.10: One dimensional flow channel connecting injection well and production well [3]

The concentration C of the tracer is modelled by [3]:

$$\frac{\partial C}{\partial t} + u\frac{C}{\partial x} - D\frac{\partial^2 C}{\partial x^2} = 0 \tag{2.13}$$

The theoretical response

$$C(t) = \frac{4M}{Q}\frac{1}{2\sqrt{\pi D t}}\exp\left(-\frac{x-4t}{4Dt}\right) \tag{2.14}$$

is simulated with the tracer data to obtain the flow channel volumes $Ax\phi$ and the longitudinal dispersivity α_L [3]. In equation (2.13, 2.14) $u = \frac{q}{\rho A\phi}$, $D = \alpha_L u$, Q is the production rate of the production well.
The software TRINIV included in the ICEBOX software package developed at Iceland geosurvey uses a non linear least squares fitting to simulate data and return the flow channel volumes and the dispersivity [3]. Ones equation (2.14) is fully defined, the concentration profile $C(t)$ can be use to determine the arrival time of the tracer concentration.

Chapter 3

Thermal front velocity in geothermal systems

3.1 Sumary

The injection of cold fluid into hot geothermal reservoirs can be formulated in terms of conservation laws. The cold front velocity induced during injection has been computed by Stopa and Wajnarowski in [57]. Their result was obtained from conservation of energy and the method of characteristics, applied to an initial boundary value problem. This computed thermal front velocity is expressed as a weighted average of the derivative of the flux function. In this paper we present a new method for computing the thermal front velocity by solving the Riemann problem. We show that the unique solution of the Riemann problem moves at the speed equal to the thermal front velocity. This result is predicted by the theory of hyperbolic conservation laws and is computed from the Rankine-Hugoniot shock condition. It is expressed as the average value of the derivative of the flux function over the interval defined by the injected water temperature and the reservoir temperature. A relative error of magnitude 10^{-3} was observed between the two results .

3.2 Introduction

In geothermal energy extraction, reinjecting colder fluid into a hot reservoir is an integral part of resource management [8, 10]. Due to the cold temperature of the injected fluid, However, cooling of the production wells can occur, as observed in Beowawe, Nevada and the Geysers Geothermal reservoir in the US [61], [60]. To mitigate this cooling effect, predicting the velocity of the cold water movement, is an essential part of the reinjection scheme. Bodvarsson [19] derived the thermal front velocity for constant fluid and rock properties, using the characteristic method. This technique produces a non physical solution when the rock and fluid properties are temperature dependent. By using the method of characteristics, Stopa and Wajnarowski solved an initial-boundary value problem for the conservation laws [57]. They derived the thermal front velocity using conservation of energy.

By formulating the injection problem as the well-posed Riemann problem, we relied on the established theory of hyperbolic conservation laws. Rather than using the method of characteristics, we used the unique solution for the Riemann problem given in [39]. This solution propagates at a speed equal to the thermal front velocity.

In this work we revisit the findings of Stopa and Wajnarowski in [57]. In particular we compare the thermal front velocity obtained in [57] with the one predicted by the theory of hyperbolic conservation laws.

3.3 Governing equation

A single phase(liquid) fluid flow in porous medium is given respectively by the conservation of mass and energy equation [63]

$$\frac{\partial(\phi\rho_w(u))}{\partial t} + \frac{\partial}{\partial x}(\rho_w(u)u_w) = 0 \tag{3.1}$$

$$\phi\frac{\partial}{\partial t}\left(\phi\rho_w(u)c_w(u)u + (1-\phi)\rho_r(u)c_r(u)u\right) + \frac{\partial}{\partial x}(\rho_w(u)c_w(u)u_w u) = \lambda\frac{\partial^2 u}{\partial x^2} \tag{3.2}$$

where u is the temperature, $c_w(u), c_r(u), \rho_w(u), \rho_r(u)$ are the heat capacity of water/rock and density of water/rock respectively. ϕ, u_w, λ are the porosity, the Darcy velocity of liquid phase and the heat conduction coefficient respectively. Darcy velocity u_w is normally pressure dependent. Therefore equations (3.1, 3.2) represent a system of two equations with two unknowns.

To simplify the system of equations (3.1, 3.2). we expend (3.2) then use the conservation of mass (3.1) to get one equation. See [57] for details. By expending (3.2) we get

$$\begin{aligned} c_w(u)u\left(\frac{\partial\phi\rho_w(u)}{\partial t}+\frac{\partial}{\partial x}(\rho_w(u)u_w)\right)+\frac{\partial}{\partial t}((1-\phi)\rho_r(u)c_r(u)u) \\ +\phi\rho_w(u)\frac{\partial}{\partial t}(c_w(u)u)+\rho_w(u)u_w\frac{\partial}{\partial x}(c_w(u)u)=\lambda\frac{\partial^2 u}{\partial x^2}0. \end{aligned} \tag{3.3}$$

Using (3.1), the first expression in (3.3) vanishes and we get

$$\frac{\partial}{\partial t}((1-\phi)\rho_r(u)c_r(u)u)+\phi\rho_w(u)\frac{\partial}{\partial t}(c_w(u)u)+\rho_w(u)u_w\frac{\partial}{\partial x}(c_w(u)u)=\lambda\frac{\partial^2 u}{\partial x^2}. \tag{3.4}$$

Applying the chain rule on (3.4) and assuming that Darcy velocity u_w is constant, after rearranging the terms we end up with

$$\frac{\partial u}{\partial t}+\frac{u_w}{\phi}F(u)\frac{\partial u}{\partial x}=\left(\frac{\lambda}{(1-\phi)\left(\frac{\partial(\rho_r(u)c_r(u)u)}{\partial u}\right)+\phi\rho_w(u)\left(\frac{\partial(c_w(u)u)}{\partial u}\right)}\right)\frac{\partial^2 u}{\partial x^2} \tag{3.5}$$

or

$$\frac{\partial u}{\partial t}+\frac{\partial G(u)}{\partial x}=\left(\frac{\lambda}{(1-\phi)\left(\frac{\partial(\rho_r(u)c_r(u)u)}{\partial u}\right)+\phi\rho_w(u)\left(\frac{\partial(c_w(u)u)}{\partial u}\right)}\right)\frac{\partial^2 u}{\partial x^2} \tag{3.6}$$

where

$$G(u)=\frac{u_w}{\phi}\int_0^u F(x)\mathrm{d}x$$

$$F(u) = \frac{\phi\rho_w(u)\left(\frac{\partial(c_w(u)u)}{\partial u}\right)}{(1-\phi)\left(\frac{\partial(\rho_r(u)c_r(u)u)}{\partial u}\right) + \phi\rho_w(u)\left(\frac{\partial(c_w(u)u)}{\partial u}\right)} \tag{3.7}$$

and from [57]

$$c_w(u) = \frac{1}{0.00023749816 + 8.0681767 * 10^{-8}u - 8.0367134 * 10^{-10}u^2}$$

$$c_r(u) = 1234.257 - 454.546\exp(-0.00397334833482u)$$

$$\rho_w(u) = 1043.196 - 42.966623\exp(0.00689550122u)$$

$$\rho_r(u) = \frac{2650}{1 + (u-20)0.5 * 10^{-4}}.$$

If we neglect conduction as second order effect by setting $\lambda = 0$ in (3.6), we get

$$\frac{\partial u}{\partial t} + \frac{\partial G(u)}{\partial x} = 0 \tag{3.8}$$

Equation (3.8) is a hyperbolic conservation laws and is the same equation derived in [57]. Function $G(u)$ is called the flux function of the scalar hyperbolic conservation laws. Equation (3.8) describe transport phenomenon. In this case transport of heat. Recall that $u = u(x,t)$ is the temperature and according to (3.8) the temperature is conserved. To see this, we can integrate over a given closed interval $[a, b]$ and get:

$$\frac{\partial}{\partial t}\int_a^b u(x,t)\mathrm{d}x = \int_a^b \frac{\partial}{\partial t}u(x,t)\mathrm{d}x \tag{3.9}$$

$$= -\int_a^b \frac{\partial}{\partial x}G(u(x,t))\mathrm{d}x \tag{3.10}$$

$$= G(u(a,t)) - G(u(b,t)) \tag{3.11}$$

$$= [inflow \quad at \quad a] - [inflow \quad at \quad b] \tag{3.12}$$

Therefore the physical quantity modelled by u, is neither created nor destroyed: The total amount of u contained inside any given interval $[a, b]$ can change only due to the flow of u across boundary points a, b.

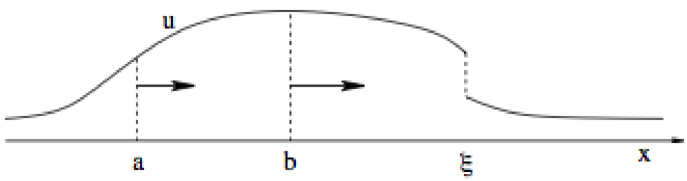

FIGURE 3.1: Flow across point a and b with discontinuity at ξ

It is well known from the literature that equation of type (3.8) admit discontinuous solutions [39]. Assume now that u has a jump or discontinuity at ξ see Figure 3.1. Then (3.8) is meaningful only in a class of discontinuous or generalised functions. Solutions must therefore be interpreted in distributional sense. We therefore say that u is a solution of (3.8) if

$$\int\int (u\phi_t + G(u)\phi_x)\mathrm{d}x\mathrm{d}t = 0 \tag{3.13}$$

for every infinitely continuous differentiable function ϕ with compact support. Equation (3.13) is the weak formulation of (3.8). We only required that u and $G(u)$ be locally integrable. This is a weaker requirement then continuity. To sum up, the problem of injecting colder water into a hot geothermal reservoir can be modelled by

$$\frac{\partial u}{\partial t} + \frac{\partial G(u)}{\partial x} = 0 \tag{3.14}$$

with initial data

$$u(x, 0) = u_0(x) \tag{3.15}$$

This model assumed that the geological formation exhibit mainly micro permeability due to very small inter granular openings [19]. This mean that the reservoir is assumed homogeneous isotropic porous and permeable media, saturated with incompressible fluid. The fluid percolating through the reservoir rock. At any given point, the fluid and the reservoir have the same temperature.

This problem was first studied by Bodvarsson for temperature independent fluid and rock properties [19]. He found that the temperature field was transported through the porous media at a rate given by the thermal front velocity.

3.4 Thermal front velocity

3.4.1 Formulation of the problem and early work

We consider a geothermal reservoir with temperature u_r and a flash water from geothermal power plant of temperature u_l. Assume that $u_l < u_r$. The flash water is injected into the reservoir. We are interested in finding the rate at which the colder injected water propagates through the reservoir. Ultimately we can calculate the distance traveled by the cold injected water with time. The thermal front velocity is defined as the rate at which the cold injected fluid moves through the reservoir rock.

Bodvarsson formulated this problem for constant rock and fluid properties [19] by

$$\frac{\partial u}{\partial t} + w\frac{\partial u}{\partial x} = 0$$

with solution

$$u = f(x - wt)$$

which means that the temperature filed is translated with velocity w (thermal front velocity), given an initial data

$$u(x, 0) = f(x)$$

In the injection problem the initial data $f(x)$ is given as a step function see figure 3.2. Due to the simplicity of the problem, he was able to apply this method to cylindrical and spherical symmetric flow.

Since solution of (3.8) admit discontinuities, practically the thermal front velocity is the velocity of the discontinuity solution.

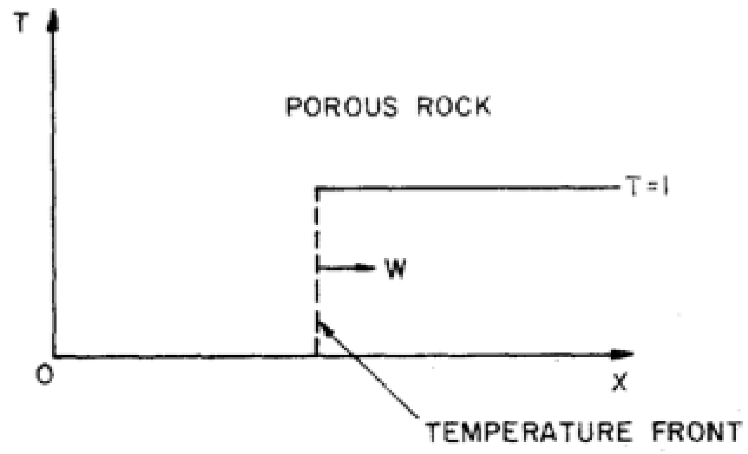

FIGURE 3.2: Thermal front moving with velocity w through a porous rock

Two cases can be considered. In the first case the rock and fluid properties are assumed constant. In this case equation (3.14) becomes:

$$\frac{\partial u}{\partial t} + \left(\frac{u_w}{\phi} \frac{\phi \rho_w c_w}{(1-\phi)\rho_r c_r + \phi \rho_w c_w} \right) \frac{\partial u}{\partial x} = 0 \tag{3.16}$$

By applying the method of characteristics, Stopa and Wajnarowki [57], derived the thermal front velocity v_{TF}:

$$v_{TF} = \frac{u_w}{\phi} \left(\frac{\phi \rho_w c_w}{(1-\phi)\rho_r c_r + \phi \rho_w c_w} \right) \tag{3.17}$$

In the second case the fluid and rock properties are temperature dependent. Equation (3.14) is therefore nonlinear and the method of characteristics fail to give a physical solution [39, 57], see Figure 3.3.

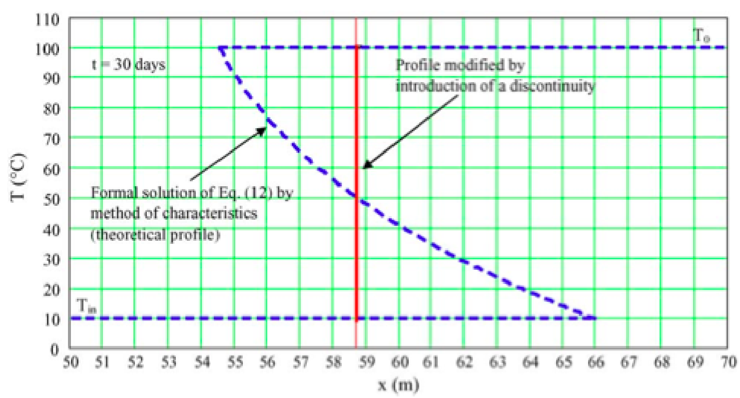

FIGURE 3.3: Non physical solution obtained in [57] from the method of characteristics

In this case The solution of equation (3.14) with initial data (3.15) see [57] is multivalued which mean that the solution is discontinuous. To obtain a physically acceptable solution, a discontinuity was inserted in the solution at position z such that conservation of energy was satisfied see Figure 3.3:

$$t\frac{u_w}{\phi}\int_{u_l}^{u_r} U(u)F(u)\mathrm{d}u = z\int_{u_l}^{u_r} U(u)\mathrm{d}u \tag{3.18}$$

setting $v_{TF} = \frac{z}{t}$ they obtained

$$v_{TF} = \frac{u_w}{\phi}\left(\frac{\int_{u_l}^{u_r} U(u)F(u)\mathrm{d}u}{\int_{u_l}^{u_r} U(u)\mathrm{d}u}\right) \tag{3.19}$$

$$U(u) = (1-\phi)\rho_r(u)(u)c_r(u) + \phi\rho_w(u)c_w(u). \tag{3.20}$$

with $U(u)$ given in Figure 3.4. The thermal front velocity obtained by Stopa and Wajnarowski is the weighted average of the derivative of the flux function :

$$G(u) = \frac{u_w}{\phi}\int_0^u F(x)\mathrm{d}x \implies \frac{dG(u)}{du} = \frac{u_w}{\phi}F(u)$$

So that (3.19) ca be written as

$$v_{TF} = \left(\frac{\int_{u_l}^{u_r} U(u)G'(u)\mathrm{d}u}{\int_{u_l}^{u_r} U(u)\mathrm{d}u}\right) \tag{3.21}$$

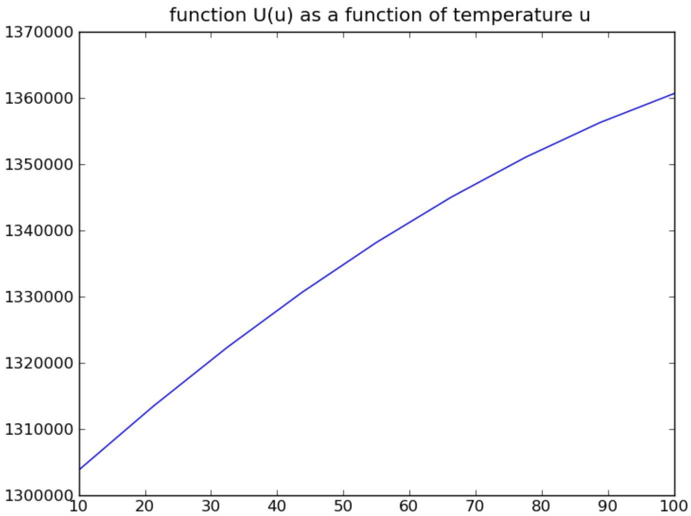

FIGURE 3.4: Function U given in 3.20

3.4.2 Thermal front velocity predicted by the theory of conservation law

Injecting colder water into a hot geothermal reservoir can be formulated as a Riemann problem : Find the unique weak solution u of

$$\frac{\partial u}{\partial t} + \frac{\partial G(u)}{\partial x} = 0, \quad u(x,0) = g(x) \tag{3.22}$$

$$g(x) = \begin{cases} u_l & \text{if } x \leq 0 \\ u_r & \text{if } x \geq 0 \ . \end{cases}$$

satisfying the Rankine-Hugoniot shock condition and the Kruzkov entropy condition. The shock condition gives the speed s of the discontinuity solution of (3.22):

$$s = \frac{G(u_r) - G(u_l)}{u_r - u_l} \tag{3.23}$$

The Kruzkov entropy condition:

$$\int_0^T \int_{-\infty}^{\infty} (\mid u-k \mid \varphi_t + q(u,k)\varphi_x)\,\mathrm{d}x\mathrm{d}t + \int \mid u(x,0)-k \mid \varphi(x,0)\mathrm{d}x \geq 0 \quad (3.24)$$

is the extra condition satisfy by the unique solution of (3.22) see [39] for detail. $q(u,k) = sign(u,k)(G(u)-G(k))$, k is a non negative constant and φ is any non negative test function.

From [39], the unique solution of (3.22) satisfying the Rankine-Hugoniot condition and the Krizkov entropy condition is:

$$u(x,t) = \begin{cases} u_l & \text{if } x \leq G'_{\cup}(u_l)t, \\ (G'_{\cup})^{-1}(\frac{x}{t}) & \text{if } G'_{\cup}(u_l)t \leq x \leq G'_{\cup}(u_r)t \\ u_r & \text{if } x \geq G'_{\cup}(u_r)t \end{cases} \quad (3.25)$$

If $u_l < u_r$, and:

$$u(x,t) = \begin{cases} u_l & \text{if } x \leq G'_{\cap}(u_l)t, \\ (G'_{\cap})^{-1}(\frac{x}{t}) & \text{if } G'_{\cap}(u_l)t \leq x \leq G'_{\cap}(u_r)t \\ u_r & \text{if } x \geq G'_{\cap}(u_r)t \end{cases} \quad (3.26)$$

if $u_l > u_r$, where $G_{\cup,\cap}$ is the lower and the upper convex envelope of G respectively.

When fluid and rock properties depend continuously on temperature, The flux function G is given by

$$G(u) = V_w \int_0^u F(\theta)\mathrm{d}\theta$$

with

$$F(u) = \frac{\phi\rho_w(u)\left(\frac{\partial(c_w(u)u)}{\partial u}\right)}{(1-\phi)\left(\frac{\partial(\rho_r(u)c_r(u)u)}{\partial u}\right) + \phi\rho_w(u)\left(\frac{\partial(c_w(u)u)}{\partial u}\right)} \quad (3.27)$$

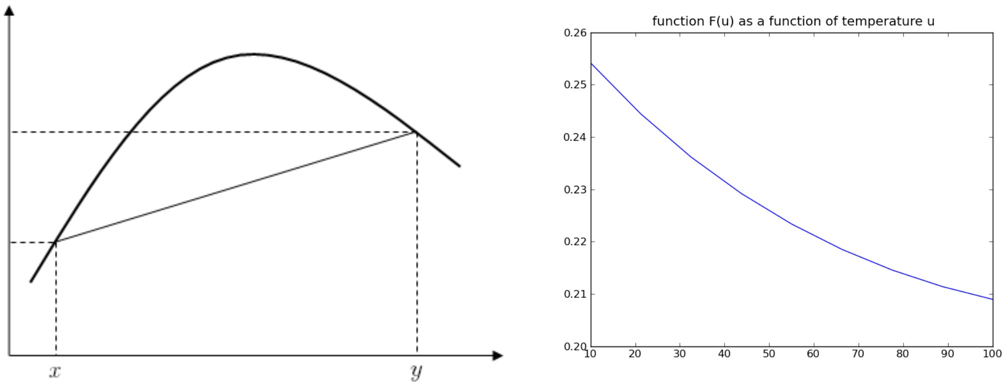

FIGURE 3.5: Function F and G with temperature $(x = u_l, y = u_r)$

From figure 3.5 F is monotonically decreasing on $[u_l = 10, u_r = 100]$, therefore the flux function G is concave on that interval. The lower convex envelope $G_{\cup}$ of G is the line passing through the points $(u_l, G(u_l))$ and $(u_r, G(u_r))$. In this case the unique solution of (3.22) moving at the speed $s = V_{TF}$ is given by

$$u(x,t) = \begin{cases} u_l & \text{if } x \leq st \\ u_r & \text{if } x \geq st \ . \end{cases}$$

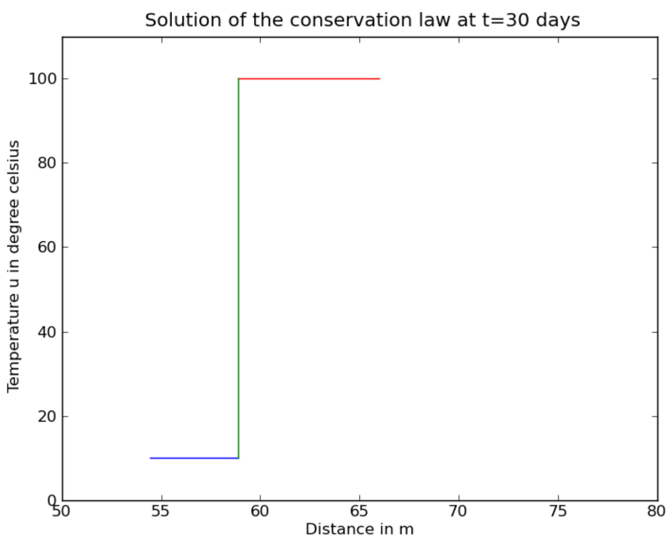

FIGURE 3.6: Solution of 3.22 at $t = 30$ days

with $s = V_{TF}$ given by the Rankine-Hugoniot shock condition

$$\begin{aligned} s &= v_{TF} \\ &= \frac{G(u_l) - G(u_r)}{u_l - u_r} \\ &= \frac{\frac{u_w}{\phi}}{(u_r - u_l)} \left(\int_0^{u_r} F(u)\mathrm{d}u - \int_0^{u_l} F(u)\mathrm{d}u \right) \\ &= \frac{\frac{u_w}{\phi}}{(u_r - u_l)} \left(\int_0^{u_l} F(u)\mathrm{d}u + \int_{u_l}^{u_r} F(u)\mathrm{d}u - \int_0^{u_l} F(u)\mathrm{d}u \right) \\ &= \frac{1}{(u_r - u_l)} \left(\int_{u_l}^{u_r} \frac{u_w}{\phi} F(u)\mathrm{d}u \right) \end{aligned} \tag{3.28}$$

3.4.3 Numerical values and discussion

In this section we compared numerically the values of the thermal front velocity from [57] and the theory of conservation laws.

u_l	u_r	[V_{TF} from (3.28) ,$10^{-5} m/s$]	[v_{TF} for (3.19), $10^{-5} m/s$]	[$V_{TF} - v_{TF}$]
10	100	2.261	2.257	$4 * 10^{-8}$
55	100	2.15	2.15	0.0
10	55	2.370	2.369	10^{-8}
20	80	2.271	2.269	$2 * 10^{-8}$
30	70	2.264	2.263	10^{-8}
40	60	2.260	2.259	10^{-8}

Table 3.1: approximated values for evaluating (3.28) and (3.19)

The thermal front velocity predicted by the theory of conservation laws is slimly higher than the one obtained by Stopa and Wajnaroski in [57]. A relative error of 10^{-3} is observed between the two results.

Chapter 4

Lumped parameters modelling in Munadarnes geothermal system

4.1 Munardanes low temperature system

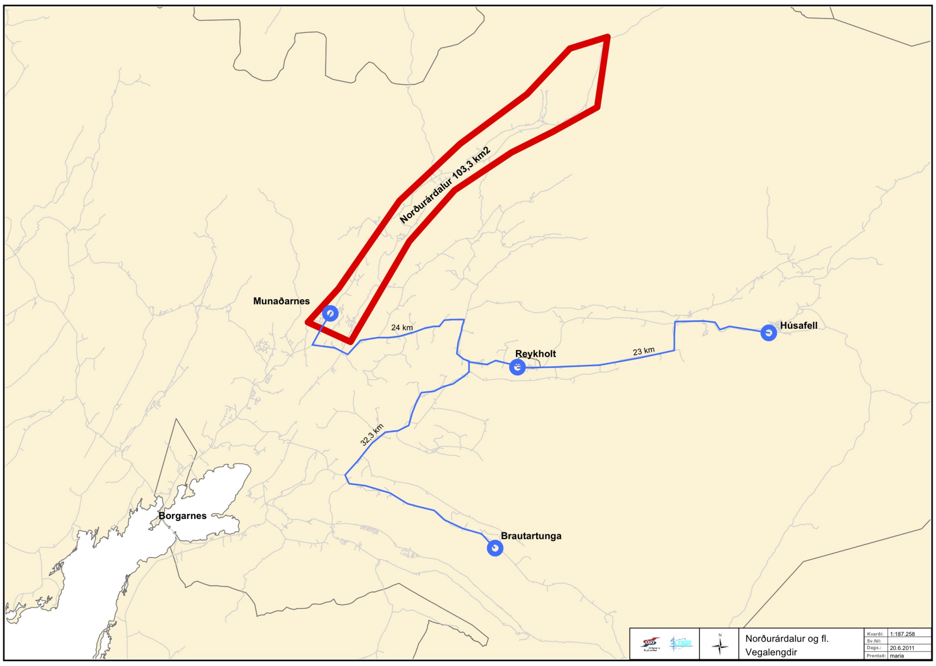

FIGURE 4.1: Borgarfjordur thermal field and Nordurardalur thermal system

The Munardanes reservoir is situated in the Nordurardalur geothermal field. The later is located in west Iceland in the Borgarfjordur thermal field situated in the

Borgarfjordur region. The Borgarfjordur thermal field is the largest low temperature geothermal field in Iceland. It comprises known thermal systems such as the Reykholt thermal system, the Bear thermal system, the Brautartunga thermal system, England thermal system, and the Husafell thermal system (Johannesson et al. 1980, Gunnlaugsson 1980). The natural discharge of the Borgarfjordur thermal system also called the Reykholtsdalur thermal system is estimated to $450l/s$ of boiling water (Georgsson et al. 1984). Within the Borgarfjordur thermal field, the Reykholf thermal system is by fare the largest thermal system with a total discharge of $400l/s$ (Georgsson et al. 1980). The Nordurardalur thermal system is located north-west to the five major thermals systems mention above. It is a N-W long band of about 103 km^2 .

4.1.1 Geological setting

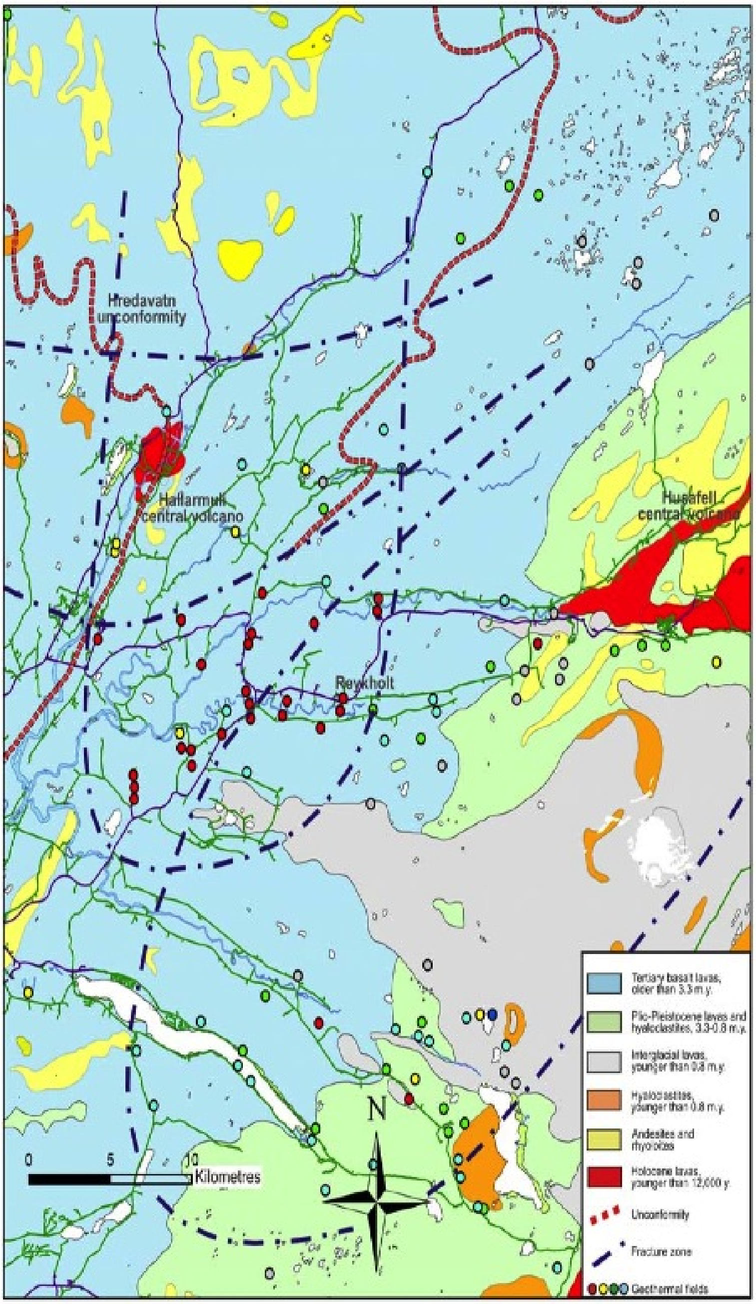

FIGURE 4.2: Geological map of Borgarfjordur thermal field

Upper tertiary (>3.3 Myr) basaltic lava flow constitute the basement of the Borgarfjordur region. This lava flow is characterised by a uniform lithology, either uniform texture or composition. The oldest rock being 14-15 Myrs. The bulk of this tertiary lava flow is made of tholeiites basaltic rock separated by minor clastic interbeds (Saemundsson, 1979). The tholeiites basaltic lava pile is characterized by its content in sodium which is less than other basaltic rock. The Borgarfjordur thermal field is bounded from the east by the western volcanic rift zone and the snaefellnes volcanic zone from the west. The later present little or no rifting. Those two volcanic zones represent the origin of the tertiary lava flow. However, the tholeiites content of the lava flow suggest that the lava flow is predominantly from the Sneafellsnes volcanic flank zone.

Both unconformity and anticline structures are visible in the region. The later formed from rift relocation (Saemundsson, 1967). Recall that an anticline is defined as layers of sedimentary rock having the oldest strata in its core and forming a convex shape. An unconformity is a planar structure indicating a discontinuity in a geologicale structure due to erosive forces. The anticline axis is defined as the line of intersection of the perpendicular plane cutting the anticline in two symmetric parts. The Borganes anticline runs NE-SW (saemundsson, 1977). The lava flow dip towards the Reykjanes-Langjokull rift zone to the east of the anticline axis. The Hredavatn unconformity is situated in north of Hredavatn lake. This unconformity indicate intense erosive forces acting in the borgarfjordur region.

4.1.2 Geophysical and hydrological setting

The geophysics of the region is characterised by the volcanism, the tectonic and the different forces affecting the earth crustal structure. The region is located between the Sneafellsnes volcanic flank and the Reykjanes-Langjokull volcanic rift. The later is made of the Reykjanes peninsula and the Western volcanic zone. The Reykjanes-Lanjokull rift is characterised by faulting resulting from tensional stress in the earth crust. The Nordurardalur geothermal system is confined within the WNW-ESE, N-S fractures zone and between the Hradavatn unconformity and the Borganes anticline. An extinct central volcano is sitting within the Nordurardalur thermal system.
The resistivity in Nordurardalur alternate between 20 and 100 Ωm. The 20 Ωm resistivity part is located in the lowest part of the Nordurardalur band and quickly increase to 60 and 100 as we move North east. The value alternate to 30-40 then decrease to 20 before increasing to about 30 Ωm.

The geothermal water is of meteoric origin which as fallen as precipitation on the highland. The water percolate through fractures cracks or others pathways through the earth and is heated by regional heat flow. The flow pattern can be infer base on preview studies done in the main thermal systems in Borgafjordur. The Northeasterly faults are the main channels for the Nordurardalur thermal system and the seismicity in the region allows fractures to serve as flow path. The recharge zone is the Arnarvatnsheidi highland and the flow pattern is

4.1.3 Proposed conceptual model of Borgarfjordur thermal filed

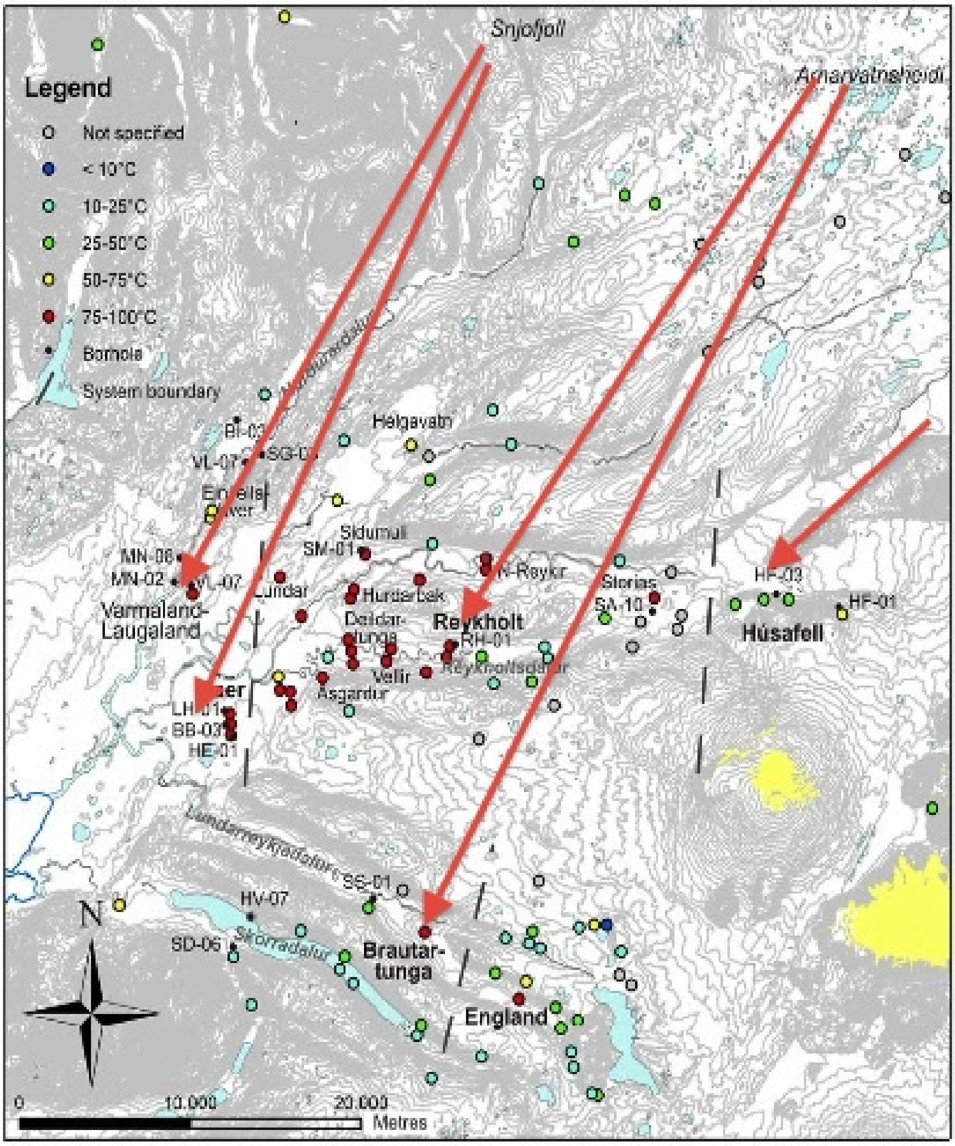

FIGURE 4.3: Production well in Borgarfjordur thermal field with flow patterns of the main thermal systems

Figure (4.3) indicates the flow patterns of the main thermal system in Borgarfjordur thermal field. The Reykholt and the Brautartungar thermal field recharge zone is located in the Arnarvatnsheidi high land. The Husafell thermal system recharge zone is located east to the Arnarvatnsheidi high land. For those tree systems, the easterly and north easterly faults and fractures allows the meteoric water to percolate at depth, acting as flow channels. The Nordurardalur system can be seen as a part of the Bear thermal system. The recharge zone is situated in the surrounding of Snjofjoll, latitude 64 Degree 59 mn N, longitude 21 Degree 11 mn W. The NS fractures act as flow channels, where the water flows by the Hallarmuli extinct central volcanoes.

Heat is transfer by conduction through the earth crust from the Snaefellsnes volcanic flank and the Reykjaness-Langjokull volcanic rift zone. Heat is convected by the hot water though the fracture and fault systems at depth. The integrity of the fracture/fault system are maintain by the seismicity in the region. They also act as barriers zone. The salinity of water is the highest in the Bear thermal system as well as in the Nordurardalur system. As we move away from the Bear system the salinity decreases, being the lowest in Husafell thermal system.

4.2 Lumped parameter modelling

Lumped parameter modelling is a cost effective high precision modelling approach for geothermal systems. It is used to simulate water level or pressure change due to production in a geothermal reservoir. By using a nonlinear iterative least square technique, the computer program LUMPFIT fit automatically the analytical response functions of lumped model to the measured data (water level or pressure), [12]. In the lumped model, the geothermal system is represented by tanks, characterised by storage coefficient κ and conductor σ, simulating respectively the storativity s and permeability K. In this modelling process the reservoir is divided into three parts if necessary. For two dimensional flow as in this work, the fluid turbulence coefficient is neglected.

Each part is approximated by a cylindrical tanks with defined radius. The inner cylinder (inner tank) is the production part which is intersected by the production well. Adjacent to inner cylinder is an intermediaries cylinder defining the interface

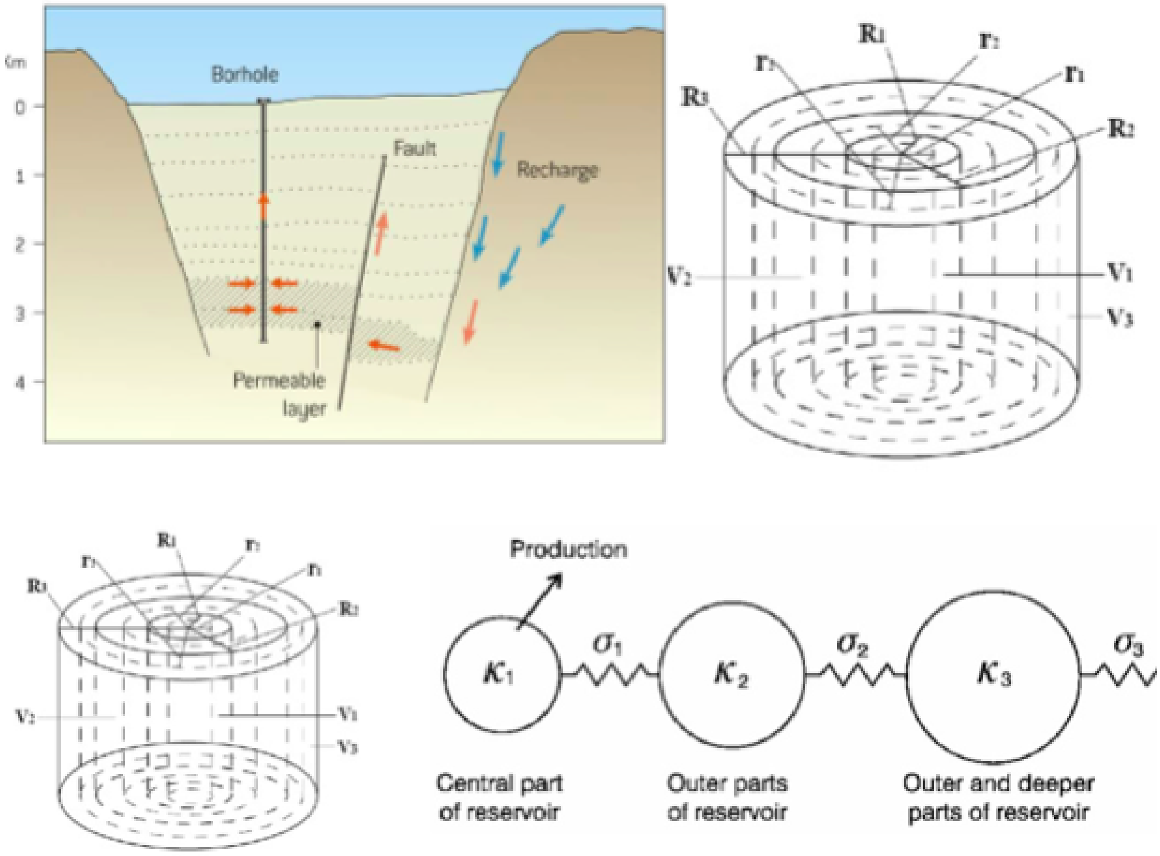

FIGURE 4.4: Subdivision of the reservoir in recharge, intermediary, and production parts

between the recharge part (outer cylinder) and the production part (inner cylinder). Each cylinder are then approximated by lumped capacitors characterised by the coefficients κ and σ simulating storativity s and permeability at the boundary of the cylinder (capacitor).

The goal is to fit the theoretical pressure response

$$P(t) = \sum Q\frac{A_i}{L_i}(1 - exp(-L_i t)) + QBt \tag{4.1}$$

$$P(t) = \sum Q\frac{A_i}{L_i}(1 - exp(-L_i t)) \tag{4.2}$$

to a set of measured water level data, for an open system and a closed system respectively. Recall that a geothermal system is open when sufficient fluid flow through it boundaries to allow recharge. The opposite is true for a closed system.

The parameters A_i, L_i, B, are function of κ_i and σ_i. After evaluating the unknown parameter (A_i, L_i, B,κ_i and σ_i), equations (4.1, 4.2) can be used to simulate and predict water level change in time. The size A, the depth H, the approximate permeability K, the storativity s and the recharge mechanism of the reservoir can also be evaluated and understood using

$$\kappa_i = V_i s = A_i H s \tag{4.3}$$

$$K = \sigma_i \frac{ln(r_{i+1}/r_i)\nu}{2\pi H} \tag{4.4}$$

$$r_1 = R_1/2, \quad r_2 = R_1 + (R_2 - R_1)/2, \quad r_3 = R_2 + (R_3 - R_2)/2 \tag{4.5}$$

$$R_1 = \sqrt{V_1/\pi H}, \quad R_1 = \sqrt{(V_1 + V_2)/\pi H}, \quad R_1 = \sqrt{(V_1 + V_2 + V_3)/\pi H} \tag{4.6}$$

4.2.1 Lumped parameter modelling of well $MN08$ in Munadarnes in Nordurardalur

Well $MN8$ was drilled in 2003 east of the summer house lacerated in Munadarnes. The 900m deep low temperature well own by Reykjavik Energy was drilled after a survey revealed a temperature gradient of 250 °c/km [38]. Testing and measurement of the well from February to March 2003 revealed that the temperature of the well is approximate 90 °c and the main main feed zone is located at about 440m [38].

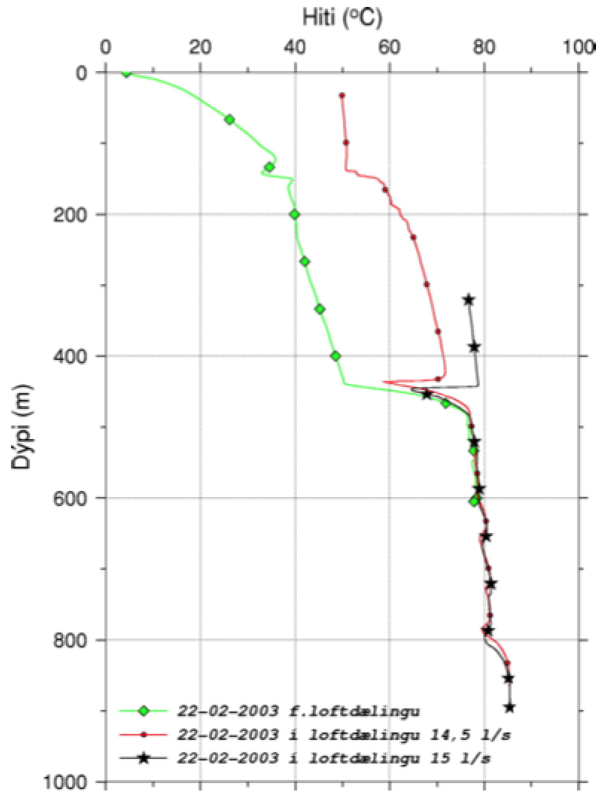

Figure 4.5: Temperature measurement in well $MN8$ [38]

Water level, pressure, temperature, production rate were monitored from January 2008 to December 2010. The well was initially drilled in 2003 with an initial water level of 35m. The first data set was rearrange by eliminating outliers, that is data points that are numerically distant from the rest of the data. The new data set was however still spread out. Despite the spreading we obtain a satisfactory two tanks open model which was later used for future prediction.

4.2.1.1 Data processing and simulation

The data obtained was very spread out. One possible explanation was that the data was contaminated by outliers.

water level in (m)	production in (l/s)	date in $(YYY/mm/dd)$	time in $(hh:mm)$
118.8	8.8	2010/03/29	11 : 23
83.6	7.1	2010/01/06	12 : 09
78.6	8.4	2009/12/01	13 : 50
76.6	8.4	2010/02/15	13 : 33
68.6	5.2	2009/02/11	10 : 20
68.6	7.3	2010/11/29	14 : 22
66.6	3	2009/10/19	9 : 40
66.6	9	2010/03/22	13 : 55
66.6	9	2010/03/24	20 : 09

Table 4.1: Outliers removed from the simulated data

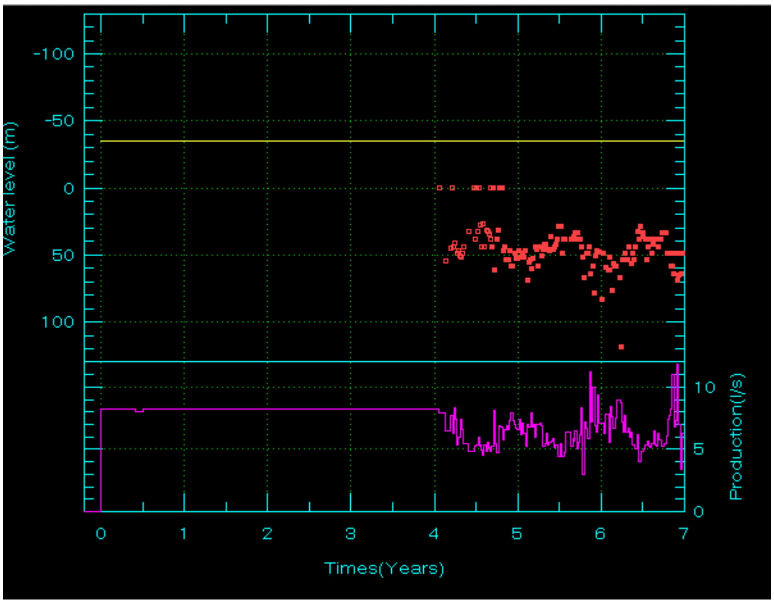

Figure 4.6: Original data set

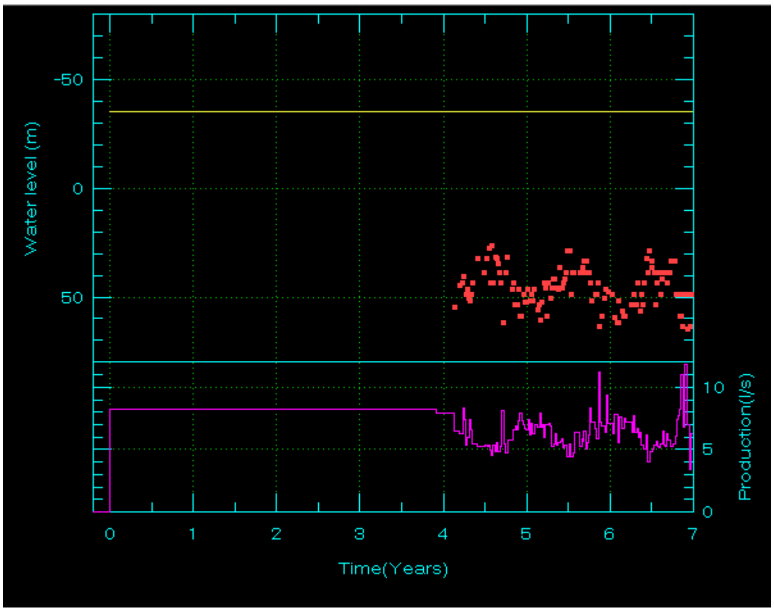

FIGURE 4.7: Data set obtained after removing the outliers in table 4.1

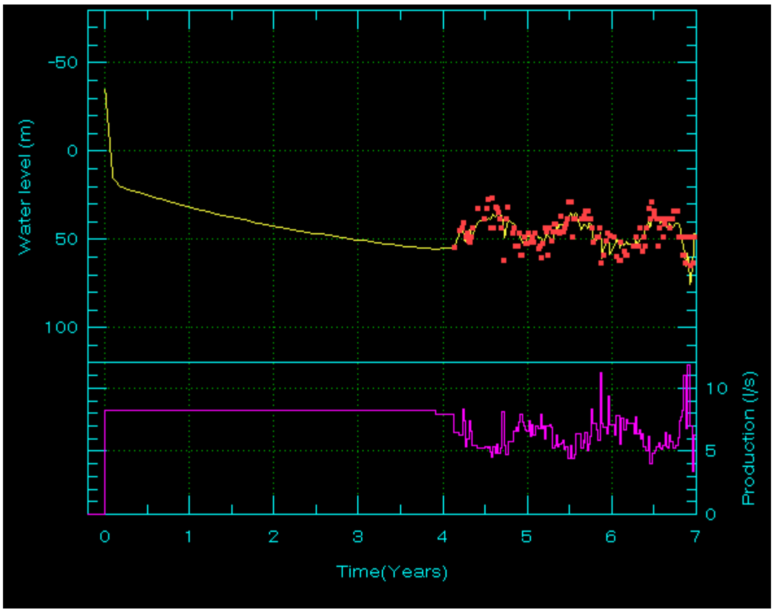

FIGURE 4.8: two tanks open model simulation

Model number	1	2	3	4
Number of tanks	1	1	2	2
Number of parameters	2	4	6	8
Model types	Closed	Open	Closed	Open
A_1	0	10.14	10.85	17.8979
L_1	0	0.8	1.16	2.82
A_2	0	0	0	0.17
L_2	0	0	0	0.025
$B\ (10^{-3})$	154.4	0	41.3	0
κ_1	1741.4	26.52	24.68	14.88
κ_2	0	0	6487.2	1593.36
κ_3	0	0	0	0
$\sigma_1(10^{-6})$	0	8	10.83	16.8
$\sigma_2(10^{-6})$	0	0	0	15.2
$RMS(m)$	12.26	7.46	6.65	5.91
$STD(m)$	12.31	7.52	6.73	6.01
$R^2(\%)$	0.00	30.6	44.88	56.46

TABLE 4.2: Parameters of the lumped models for the production well $MN8$ in Munardanes

Porosity ϕ	0.15
depth $H(m)$	900
gravity (m/s^{-2})	9.81
Water compressibility $C_w(10^{-10}Pa^{-1})$	4.6534
Rock compressibility $C_r(10^{-10}Pa^{-1})$	3.3
$s_c(10^{-7}kg/m^3Pa)$	3.4
$s(10^{-5}kg/m^3Pa)$	1.7

TABLE 4.3: Storativity estimation for well $MN8$ in Munardanes

If the reservoir was confined, it would cover an area of about $525.5km^2$ which is too large compared to the geothermal field. On the other hand, in the unconfined case, the total area for the reservoir is about $10.5km^2$. We therefore conclude that the reservoir is unconfined, with an approximated area of $10.5km^2$. The permeability is estimated at about 69.8 $mDarcy$.

4.2.1.2 Prediction with reinjection

Based on the analytical pressure response given in equation (4.2), a 20 years future prediction is given for different production scenarios.

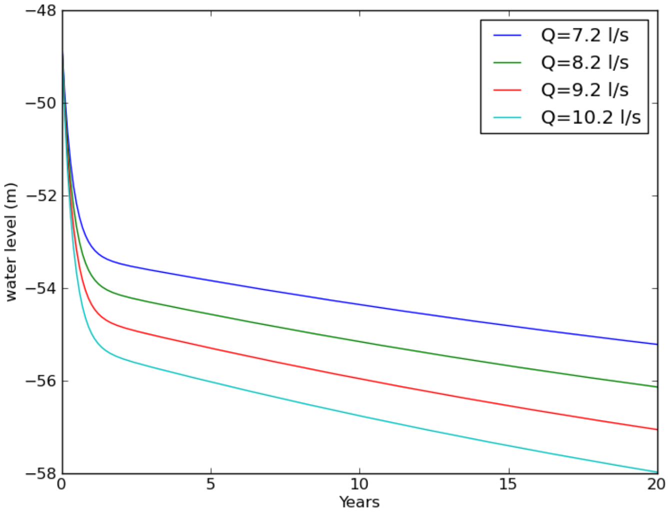

FIGURE 4.9: 20 years future prediction from 2010, without reinjection

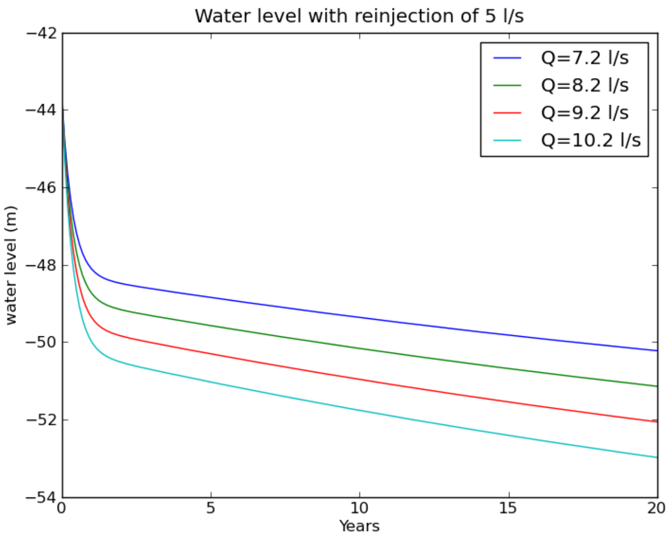

FIGURE 4.10: 20 years production with reinjection scenario for 5 l/s injection rate at the start of production

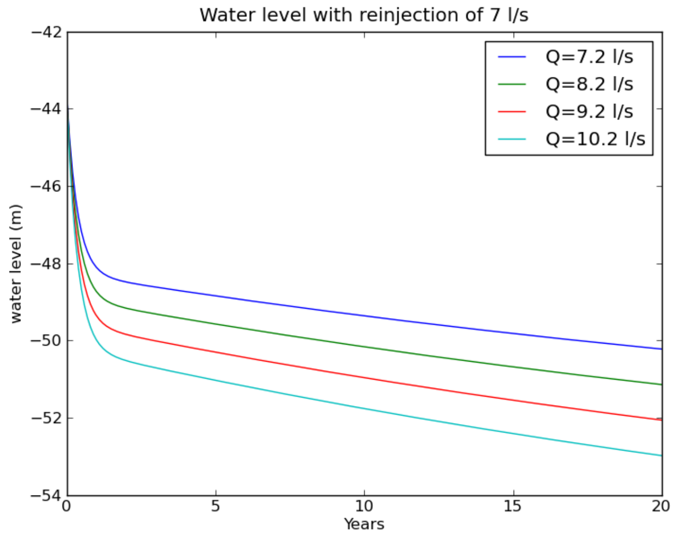

FIGURE 4.11: 20 years production with reinjection scenario for 7 l/s injection rate at the start of production

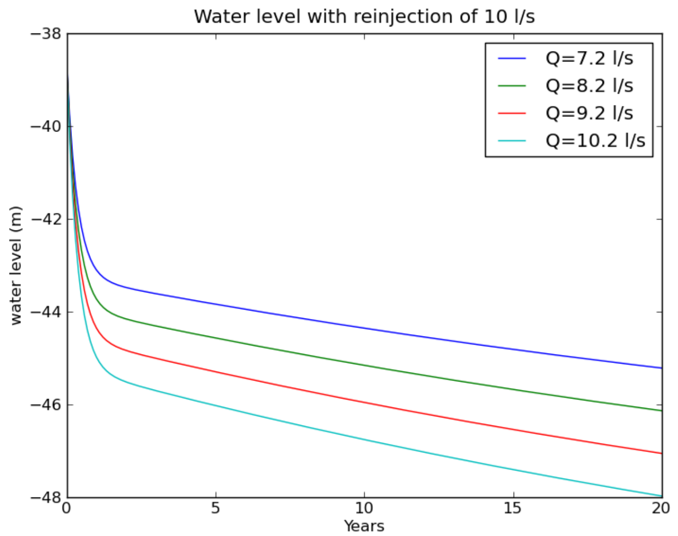

FIGURE 4.12: 20 years production with reinjection scenario for 10 l/s injection rate at the start of production

Figure 4.9 shows a 20 years prediction with production rate of 7.2 l/s, 8.2 l/s, 9.2 l/s and 10.2 l/s. Figure 4.10, 4.11 and 4.12 shows the change in water level over a period of 20 years with three injection scenarios of water at 5, 7 and 10 l/s reinjection rate. The reinjection scenarios assumed that reinjection started at the beginning of of 2004. The minimum and maximum production rate are assumed to be 7.2 l/s, 10.2 l/s respectively. As seen water leveel increases significantly with injection. However due to the cold nature of the injected water some cooling can be induce.

4.2.1.3 Location of injection well and cooling of production well

Based of a theoretical model of a one dimension flow channel, along a fracture zone, The temperature of a production well is given by [3]:

$$T(t) = T_0 - \frac{q}{Q}(T_0 - T_i)\left(1 - \left(\frac{kxh}{c_w q\sqrt{\kappa(t - x/\beta)}}\right)\right) \tag{4.7}$$

with $T(t)$ the production fluid temperature, T_0 the undisturbed reservoir temperature, T_i the injection temperature, q and Q the rate of injection and production respectively, k the thermal conduction of the reservoir rock, κ the thermal diffusivity, x the distance between injection and production wells and

$$\beta = \frac{qc_w}{< \rho c >_f hb}$$

with

$$< \rho c >_f = \rho_w c_w + \rho_r c_r(1 - \phi)$$

the volumetric heat capacity of the material in the flow channe. ρ and c are density and heat capacity respectively, with indices w and r standing for water and rock.

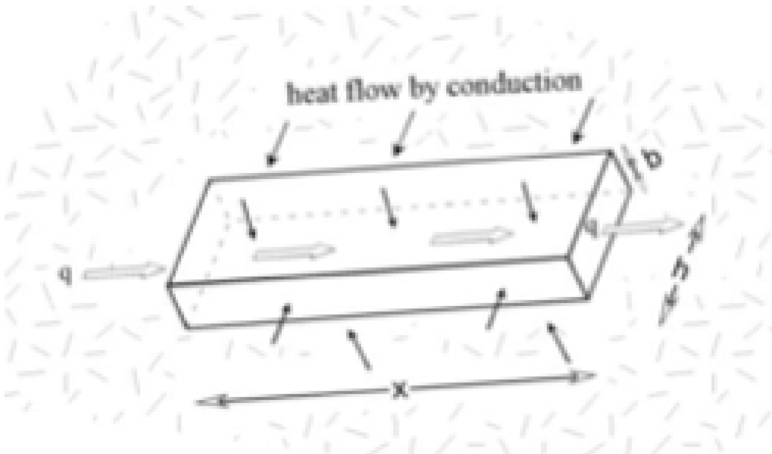

FIGURE 4.13: model of flow channel for cooling of production well during injection [3]

Assume a one dimensional channel with $h = 29\ m$, $b = 7\ m$ and porosity $\phi = 0.15$. The injection water temperature is $T_i = 20\,^{\circ}$c and the reservoir temperature $T_0 = 86\,^{\circ}$c. The thermal conductivity $k = 2$. The specific heat capacity and the density are given by Stoppa et. al as a function of temperature [57]. The theoretical cooling of well $MN08$ in Munadarnes during a 10 years reinjection scenario is given bellow:

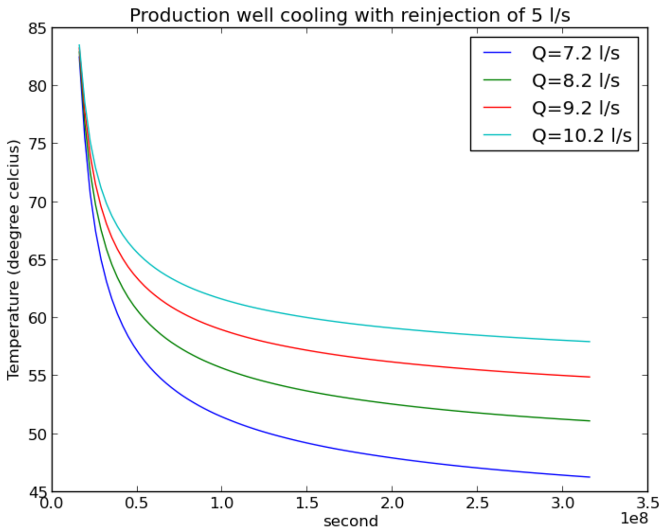

FIGURE 4.14: Production well cooling for injection well located at 500 m from production well. Injection rate 5 l/s

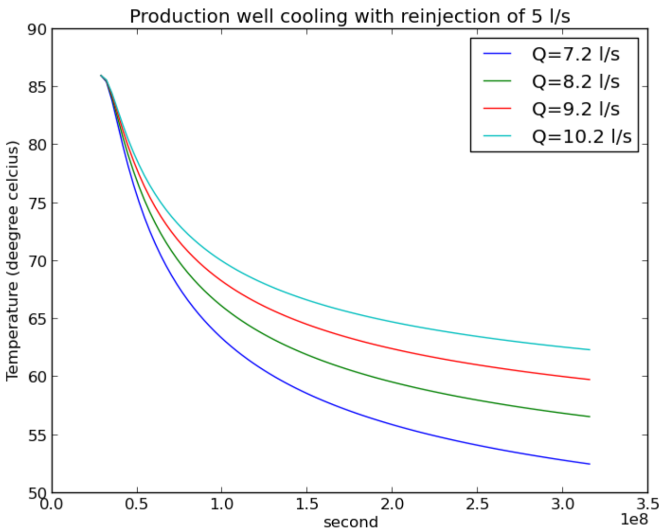

FIGURE 4.15: Production well cooling for injection well located at 1 km from production well. Injection rate 5 l/s

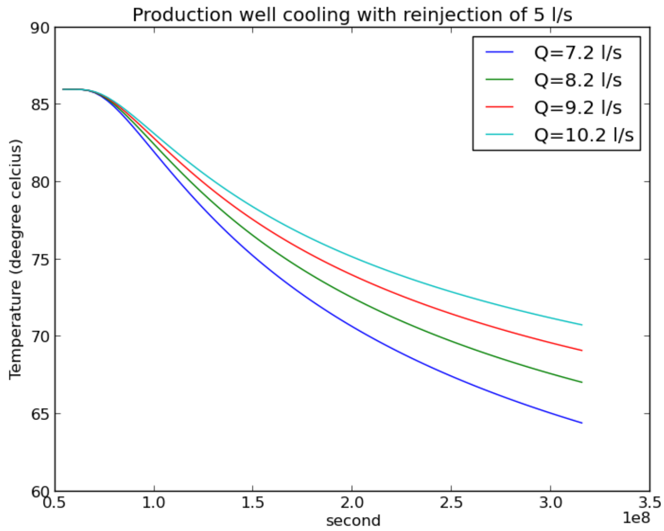

FIGURE 4.16: Production well cooling for injection well located at 2 km from production well. Injection rate 5 l/s

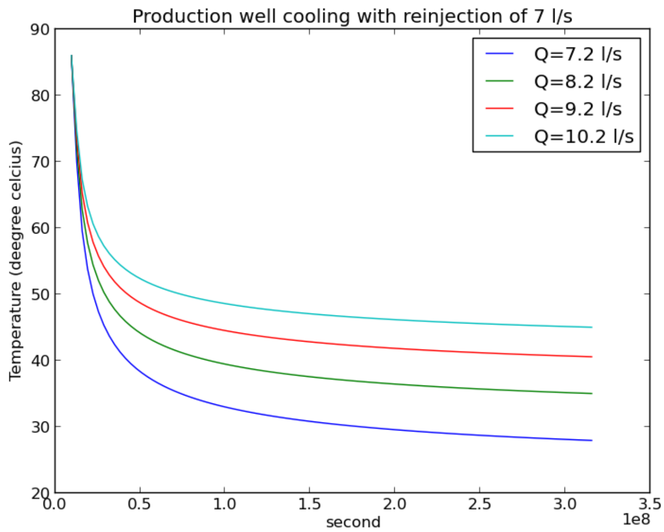

FIGURE 4.17: Production well cooling for injection well located at 500 m from production well. Injection rate 7 l/s

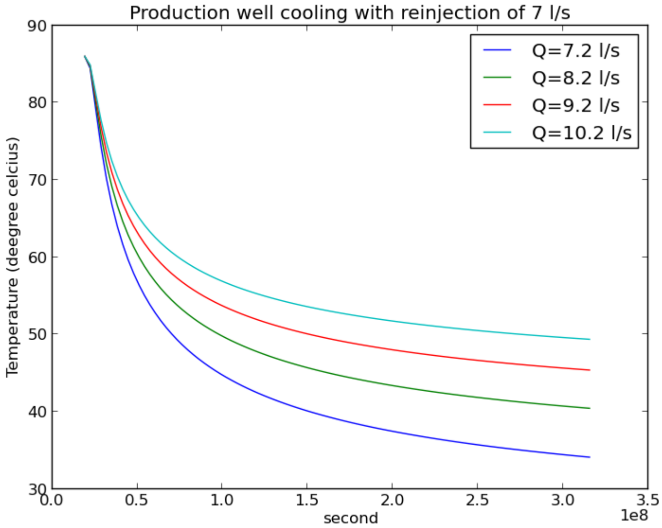

FIGURE 4.18: Production well cooling for injection well located at 1 km from production well. Injection rate 7 l/s

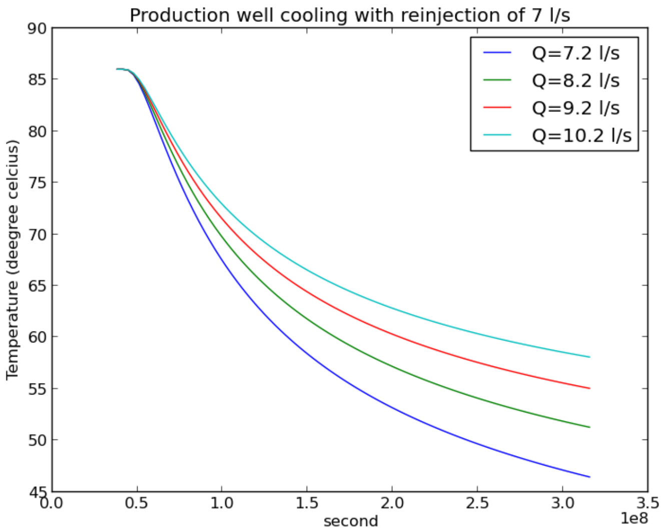

FIGURE 4.19: Production well cooling for injection well located at 2 km from production well. Injection rate 7 l/s

As seen from Figures 4.14 to 4.19 the temperature of the production well decrease when the injection well is closer to the production well. At a distance of 2 km the cooling effect is attenuated. The production well temperature is lower for higher injection rate. As the production rate is increased so is the temperature of the production well during injection.

Chapter 5

Conclusion and future work

The focus of this thesis was to model a low temperature geothermal system by using two dynamical methods: A lumped parameter modelling for simulating pressure change and an analytical method for determining the velocity of cold water movement during injection. A data set was provided by Reykjavik Energy for lumped parameter simulation of well $MN8$. The sample data consisted of water level (Pressure) and production rate from 2003 to 2008. This data appears to to be spread out, possibly due to measurement error. Using a two tanks open model the simulation was performed with a coefficient of determination of about 56 %. From the lumped parameter modelling of well $MN8$ located in Munadarnes in west Iceland, the Munadarnes reservoir permeability was estimated to be about 68.8 mD. Most geothermal system permeability is in the range of $1 - 100$ mD. The reservoir size was estimated to be about 10.5 km^2, with unconfined recharge mechanism.

Based on simulation parameters from the lumped parameters modelling, a 20 years production scenario without and with reinjection revealed that reinjecrion mitigates pressure drown down due to production. For a current production rate of 8.2 l/s and a reinjection water of $20\,^{\circ}$c a scenario without injection shows that over 20 years the water level will drop by 7.4 m. However with reinjection at a rate of 5 l/s the water level with decrease by 2.4 m. Renjecting cold water into a hot reservoir can cause the reservoir rock to cool down. To mitigate this cooling effect the injection well must be placed within the production zone and at a few km from the production well. From a theoretical solution of fluid flow in a one dimensional

channel the cooling of well $MN08$ was studied over 10 years. The cooling of well $MN08$ depends on three factors: The injection rate q, the production rate Q and the distance between the production well and the injection well. The injection rate was set at 5 l/s while the production rate varies from 7.2 to 10.2 l/s. From an initial reservoir temperature of 86 °c the temperature of the reservoir over 10 years was about 58 °c for a production rate of 10.2 l/s and a distance of 500 m between production well and injection well. When the distance between production and injection well was increased to 2 km the reservoir temperature over 10 years was about 71 °c.
For the same injection rate of 5 l/s and production rate of 7.2 l/s the temperature of the well was 46 °c and 64 °c for a distance of 500 m and 2 km respectively. This results shows that to minimise the cooling effect of reinjection the injection well must be place at few km from the production well within the production zone. increase in production rate also mitigate cooling during injection of cold water. Accurate position of injection well must however be determined after a tracer test experiment.

The velocity of the cold injected water was also derived from the theory of hyperbolic conservations laws. The result present in this work was compared with the one obtained by Stoppa et al. A relative error of 10^{-3} was observed between the two results. The numerical evaluation of the analytical expressions was derive using a simple numerical integration scheme: The trapezoidal rule.

This work can naturally be extended to include a lumped parameter modelling of hight temperature reservoirs. In this case the two phase flow nature of high temperature wells must be included. The injection of cold water in two phase flow reservoirs can also be studied. Due to the complexity of two phase flow a numerical method might be necessary.

Bibliography

[1] Achou Y.D An Effective Method to Compute Thermal Font Velocity in Geothermal Systems . *Proceedings of the 26th Nordic Seminar on Computational Mechanic, Oslo Norway 2013*

[2] Axelsson G. Stefansson V Bjornsson G. Liu J Sustainable Management of Geothermal Resources and Utilization for 100-300 y *Proceedings of the World Geothermal Congress 2005, Antalya , Turkey*

[3] Axelsson G. Bjornsson G. and Montalvo F Quatitative interpretation of tracer test and data. *Proceedings of the World Geothermal Congress 2005, Antalya , Turkey*

[4] Axelsson G. Management of Geothermal Resources. *Workshop for decision makers on direct use of geothermal resources in Asia, United Nation University*, 2008.

[5] Axelsson G. Lecture notes. *Reykjavik, Iceland. United Nation University* 2008

[6] Axelsson G. Flovenz O.G. Hauksdottir S. Hjartarson A. Liu J. Analysis of tracer test data, and injection-induced cooling, in the Laugaland geothermal field, N-Iceland *Geotermics Volume 30, 6 (2001)697-725*

[7] Axelsson G. Gunnlaugsson E Long term Monitoring of High and Low Enthalpy Field Under Exploitation. *International Geothermal Association, World Geothermal congress, 2000 short course, Kokonoe, Kyushu District, Japan, May, 226 pp*

[8] Axelsson, G. Importence of reinjection in geothermal system. *Workshop for decision makers on direct use of geothermal resources in Asia, United Nation University*, 2008.

[9] Axelsson, G. Lecture Notes Spring . *Isor , United Nation University, Iceland*, Spring 2008.

[10] Axelsson, G. Production capacity of geothermal systems. *Workshop for decision maker on direct use of geothermal resources in Asia, United Nation University*, 2008.

[11] Axelsson, B. Bjornsson, G. Raliability of Lumped Parameter Modeling of Pressure Changes in Geothermal reservoir. *Proceeding World Geothermal COngress*, Turkey, 2005.

[12] Axelsson, G. Simulation of pressure response data from geothermal reservoir by lumped parameter models. *Proceedings, Fourteenth workshop on geothermal reseevoir engineering*Standford University, Standford, 1989.

[13] Barker B.J., B.A Koenig and M.A. Stack, 1995 Water injection management for resource maximisation: Obserservation from 25 years at the Geysers, California. *Proceeding of the World Geothermal Congress 1995, Florence, Italy, May1959-1964*

[14] Baehr,H.D Heat and mass transfer,. *Springer, Berlin, Germany.*, Revised edition, 2006.

[15] Bear, Jacob. Dynamics of fluids in porous media. *Elsvier, New York*, 1988.

[16] Bilicki Z. Kestin J. Michaelides E.E Flow in geothermal wells: Part 3 Calculation Model for Self-flowing Well *Brown University. Report GEOFLO/5, DOE/ET/27225-8,Rhode Island, USA*, 1981.

[17] Bjornsson J A multi-feed zone Geothermal Wellbore Simulator. *University of California, USA* 1987.

[18] Bodvarsson, G. Swhiterspoon,P.A Geothermal reservoir engineering ,. *Geotherm. Sci and Tech., Volume 21, (1989) pp 1-68*

[19] Bodvarson, G. Thermal problem in sitting of reinjection wells,. *geothermic,1, (1972), 63-66*

[20] Bodvarson, G. G, Stefansson. Reinjection into geothermal reservoir,. *Geothermal reservoir engineering, (1988), 103-120*

[21] Bluman, G. W. Cole, J.D Similarity methods for differential equation,. *Applied Mathematical Sciences, 13, Springer-Verlag, New York Heidelberg, Berlin* 1974

[22] Brenner C. Susanne, Scott L. Ridgway The mathematical theory of finite element methods. *Springer, Third edition, New York*, 2008.

[23] Capetti G., L.Parisi, A.Ridolfi and G. Stefani(1995) Fifteen years of injection in the Larderello-Valle Secolo area:Analysis of the production data. *Proceedings of the World Geothermal Congress 1995, Florence, Italy, May, 1997-2000.*

[24] Bringedal. C Linear and nonlinear convection in porous media between coaxial cylinder. Master of science thesis in applied computational mathematics, University of Bergen, 2011.

[25] Beretta G. P World energy consumption and resources: An outlook for the rest of the century. *Dipartimento di Ingegneria Meccanica. Universita di Brescia. Italy*

[26] Bu X. Ma Weibib. Li Huashan Geothermal Energy Production Utilising Abandoned Oil and Gas Wells. *Renewable Energy 41(2012)80-85*

[27] Cheng W-L, Li T-T, Wang C-L Studies on geothermal power generation using abandoned oil wells *Energy 59(2013)248-254*

[28] Chetveryk, H. Analytical and numerical modeling of cold water injection in to Horizontal reservoir,. *Geothermal training program, The United Nation University, Iceland, 2000, Report number 4*

[29] Daryl L. Logan A first course in finite element method. *THOMSON, Canada, Fourth edition*, 2007.

[30] Edwards A.L Trump: A computer program for transient and steady state temperature distribution in multi dimensional systems *Report UCRL-14754. Rev. 3. Lawrence Livermore National Laboratory. Livermore CA. USA*, 1972.

[31] Evan, S. L Partial Differential equation,. *AMS, RHodes Island., VOLume 19* 2000

[32] Fowler, C.M.R. The solid earth: An Introduction to global geophysics *Cambridge University press, Cambridge* , 2005.

[33] Gelfang, I.M Generalized Functions,. *Academic press, New York and London. Volume 1*(1964)

[34] Gould T.L Vertical Two-Phase Steam-Water Flow in Gethermal Wells. *Journal of Petroleum Technology. 26:833-842* 1974.

[35] Grant, M. Donaldsson, I.G Geothermal Reservoir Engineering,. *Academic press, New York-USA.,1982*

[36] Gudmundsdottir H. A Coupled Wellbore-Reservoir Simulation utilizing MEasure Wellhead Conditions. *University of Iceland, Iceland*, 2012.

[37] Hagdu T, Zimmerman R. W, Bodvarsson G Coupled Reservoir-Wellbore Simulation of Geothermal Reservoir Behavior. *Geothermics, Vol, 24, No. 2.pp. 145-166*, 1995.

[38] Hjartarson A. Bjornsson G. Saemundsson K Stimulation and measurement in well MN 8 in Munadarnes. *A report prepared for Orkuveita Reykjavik by Iceland geosurvey*, 2003.

[39] Holden, H. Risebro, H.H Front tracking for Hyperbolic Conservation Laws,. *Springer, Berlin. New York-USA., 2th edition, 2007*

[40] Kocabas, I. Geothermal characterization via Thermal injection back flow and inter wells tracer testing,. *Geothermic, 34, 27-46 (2005)*

[41] Logg Anders Automated solutions of differential equations by the finite element methods. *Germany* , 20011.

[42] Narasimhan T.N, Witherspoon P.A An integral finite difference method for analysing fluid flow in porous media. *Water Resour. Res. 12.57-64*, 1976.

[43] Narasimhan Norton D.L Theory of Hydrothermal systems. *Ann. Rev. Earth Planet. Sci 1984. 12:155-77*

[44] Miller C.W Wellbore Users Manual. *Berkley University of California. Report , No LBL-10910, USA* 1980.

[45] Ockendon, J. Howinson, S Applied Partial Differential equations,. *Oxford, New York.,Revised edition*2003

[46] Olver, p.J Equivalence, Invarients, and symmetry, *Cambridge University press* 1995

[47] Osullivan, M.J, Karsten Pruess, Marcelo J Lippman State of the art of geothermal reservoir simulation. *Geothermics 30(2001). 395-429* .

[48] Pritchett J. W STAR: A geothermal simulation system. *Proceedings of the World Geothermal Congress*, 1995.

[49] Pruess K THOUGH2 Users Guide. *Version 2.0 Berkley, Univesity of California, USA*, 1999.

[50] Pruess Kasten Mathematical modeling of fluid flow and heat transfer in geothermal systems-An introduction in five lectures. *United state University, Iceland, Reykjavik* , 2002.

[51] Sayantan G. Kumar M Geothermal Reservoir- A brief Review *Journal of Geological Society of India. Vol.79, Jun 2012, pp.582-602*

[52] Stark M.A, W.T Box Jr, J.J Beall, K.P Goyal and A.S Pingol, 2005 The Santa Rosa-Geyser Recharge Project . *Geyser Geothermal Field California, Proceedings of the World Geothermal Congress 2005, Antalya, Turkey, April, 9 pp*

[53] Stefansson V., 1997 Geothermal Reinjection experience. *Geothermics, 26, 99-130*

[54] Salas, D.M The curious events leading to the theory of shock waves,. *Invited lecture at the 17th shock International symposium, Rome-Italy*(2006)

[55] Springer reference. Springer. *www.springerreference.com*

[56] Vinsome P.K.W., Shook, G.M Multi-Purpose Simulation. *Petrol Science and Engineering 9(1)29-38.*

[57] Wajnarowski, P. Stapo, S Analytical model of cold water front movement in a geothermal reservoir,. *Geothermics, 35, 59-64* (2006)

[58] Young, H.D. Fredman, R.A University physics,. *Addison Wesley, Boston, New York.,11th edition*2004

[59] Zoback, M.D Reservoir Geomechanics ,. *Cambridge University press, United Kingdom,* 2008

[60] A. Logg., *Injection at the Beowa geothermal reservoir*, Elsvier, USA, 2011.

[61] P. S. Pacheco., *Tracing of injection in the Geysers*, Elsvier, USA, 2011.

[62] Wang K., 2005 Studies of the Reinjection Tests in Basement Geothermal Reservoir, Tianjin, China. *Proceedings of the World Geothermal Congress 2005, Antalya, Turkey, April, 12 pp.*

[63] Woods. John,. P. K nobloch., *vaporisation of a liquid moving front moving through a hot rock porous medium*, Advance in computation mathematics, USA, 2007

[64] Iceland Geosurvey Iceland Geosurvey webpage *www.isor.is*

[65] US Department of energy Energy Efficiency and Renewable Energy *www1.eere.energy.gov*